The Role of Peroxisome Proliferator-Activated Receptor Gamma in Mediating the Immunomodulatory Effects of Di-n-butyl Phthalate in THP-1 Cells

Vegard Sæter Grytting

MASTER THESIS IN TOXICOLOGY

Department of Biosciences

Faculty of Mathematics and Natural Sciences

UNIVERSITY OF OSLO

2017

The role of peroxisome proliferator-activated receptor gamma in mediating the immunomodulatory effects of di-n-butyl phthalate in THP-1 cells

2017

Title: The role of peroxisome proliferator-activated receptor gamma in mediating the immunomodulatory effects of dibutyl phthalate

Author: Vegard Sæter Grytting

http://www.duo.uio.no

Print: Reprosentralen, Universitetet i Oslo

Abstract

Di-n-butyl phthalate (DBP) is considered a common contaminant in the indoor environment. Exposure to DBP has been linked to the prevalence of asthma and airway symptoms in epidemiological studies. *In vitro* studies have reported that DBP may influence immunological properties in macrophages, cells that are central to the pulmonary innate immunity and implicated in the pathogenesis of asthma. However, the mechanisms responsible for mediating these effects are currently unknown.

The present study was conducted to assess the role of the nuclear receptor peroxisome proliferator-activated receptor gamma (PPARγ) in mediating the immunomodulatory effects of DBP on macrophages, focusing on the expression of the cell surface marker CD36, which is enhanced during the differentiation of THP-1 monocytes into macrophage-like cells. The involvement of PPARγ was assessed using a combined exposure of DBP and the PPARγ agonists rosiglitazone and 15-deoxy-$\Delta^{12,14}$-prostaglandin J_2 (15d-PGJ_2), and the PPARγ antagonist GW9662. The expression of cell-surface CD36 was determined using flow cytometry analysis.

DBP enhanced the expression of CD36, although not to the same extent as the agonists rosiglitazone and 15d-PGJ_2, indicating weak agonistic properties. During combined exposure, DBP attenuated the effect of the synthetic agonist rosiglitazone on CD36 expression. In contrast, exposure to DBP in combination with the endogenous agonist 15d-PGJ_2 increased the expression of CD36 in an additive manner, compared with exposure to 15d-PGJ_2 alone. Pre-incubation with the antagonist GW9662 failed to supress the effect of DBP on CD36, while the same doses effectively blocked the effect of rosiglitazone. The reduction in the effect of rosiglitazone indicates that DBP may displace a reversibly bound agonist in the canonical ligand-binding site, while the DBP-induced increase in CD36 in the presence of the covalently bound ligands 15d-PGJ_2 and GW9662 indicates affinity for the alternative ligand-binding site.

Taking into account the structure of the PPARγ ligand-binding domain and the interactions of rosiglitazone, 15d-PGJ_2 and GW9662 with this domain, the results presented in this study point towards DBP acting as a weak partial PPARγ agonist that may activate the receptor through interactions with both the canonical and alternative ligand-binding site.

Acknowledgements

I would like to thank all of those who have helped me throughout the process of completing my thesis. My research would not have been possible without the support of my main supervisor Anette Kocbach Bølling. I am sincerely grateful for your guidance during my laboratory work and the writing process, your reassuring presence has been a tremendous help. Thanks to my assistant supervisors Jørn Andreas Holme, Johan Øvrevik and Ketil Hylland, your advice and encouragement has been invaluable to my work. I would like to express my gratitude to Hans Jørgen Dahlman and Tonje Skuland for teaching me laboratory methods imperative to my research and for being there to help whenever I required assistance or advice. Finally, I would like to thank my family and friends for their support and understanding during this laborious time.

Table of contents

1 Introduction

1.1 Background

The prevalence of asthma is currently on the rise (Asher *et al.* 2006). The disease afflicts approximately 300 million people worldwide (Croisant 2014) and is associated with a total estimated annual cost of 72.2 billion euro in EU countries (ERS 2013) and 56 billion dollars in the US (Loftus and Wise 2015). One potential contributing factor to the rise is the exposure to endocrine disruptors, such as phthalates, which may modulate the immune system and the allergic response (Chalubinski and Kowalski 2006). Phthalates are industrial chemicals that are considered ubiquitous contaminants in the indoor environment due to their widespread use in building materials and consumer products (Wormuth *et al.* 2006). Epidemiological studies have revealed a possible link between the exposure to various phthalates or the presence of plastic building materials, and adverse respiratory symptoms such asthma and allergic disease (Jaakkola and Knight 2008).

Di-n-butyl phthalate (DBP) is a commonly used phthalate that may reach high concentrations in indoor air, causing inhalation exposure (Bølling *et al.* 2013). In the airways, macrophages are prominent immune cells that are central to tissue homeostasis and the defence against pathogens. Macrophages are also implicated in the pathogenesis of asthma (Byers and Holtzman 2010, Murray and Wynn 2011, Wynn *et al.* 2013). Previous studies have suggested that DBP may alter the production of cytokines and enhance the phorbol myristate acetate (PMA)-induced expression of cluster of differentiation (CD) surface markers, like CD36, in macrophages derived from THP-1 cells (Olderbø 2015). However, the intracellular signalling pathways responsible for mediating the effects are currently unknown. This study seeks to complement the previous studies and clarify the mechanistic basis for the observed effect of DBP exposure on CD36 expression.

1.2 The respiratory system

1.2.1 The immunology of the respiratory system

The respiratory system consists of a series of structures responsible for the exchange of gasses between the blood and the atmosphere, as well as the regulation of pH homeostasis, vocalisation and the protection against inhaled pathogens and pollutants (Silverthorn 2015). It is in close contact with the external environment and therefore a prominent route of exposure to airborne pathogens, pollutants and irritating substances. Air is filtered in the upper airways, which is lined with ciliated cells covered in mucus that traps inhaled particles larger than 2 μm (Silverthorn 2015). Pathogens and particles that reach the lower airways are cleared by the complementary actions of the innate and adaptive immune system.

The innate immunity in the lung consists of both a humoral component and cellular effector functions, and is mediated by epithelial cells and resident and recruited immune cells (Zaas and Schwartz 2005). The initial line of defence consists of soluble proteins and peptides, which incapacitate the pathogen or facilitates phagocytosis by leukocytes (Zaas and Schwartz 2005). Macrophages are the most numerous leukocyte in the lung and central to the innate immunity (Martin and Frevert 2005). They are phagocytic cells and ingest all particulates, debris and microorganisms that reach the alveoli, and take part in regulating the state of inflammation in the area through the release of inflammatory and chemotactic mediators, such as cytokines and chemokines (Martin and Frevert 2005). Macrophage populations are heterogeneous and may alter their phenotype in response to different stimuli related to infection, damage or altered homeostatic conditions (Wynn *et al.* 2013, Hume 2015). They sample their surroundings using pattern recognition receptors (PRR) that interact with pathogen-associated molecular patterns (PAMP) or damage-associated molecular patterns (DAMP), recognizing infection or injury respectively (Murray and Wynn 2011).

Activated macrophages have typically been classified according to two functional categories; M1, or classically activated macrophages, and M2, also known as alternatively activated macrophages. More recently, macrophage activation has been shown to be more akin to a spectrum, in which the cells exhibit different markers and properties depending on stimulus, rather than distinct polar states (Xue *et al.* 2014,

Hume 2015). However, the terms M1 and M2 are still useful for describing macrophage function and activity. M1 macrophages are activated by interferon γ (IFNγ) and bacterial lipopolysaccharide (LPS), while M2 macrophages are activated by interleukin 4 (IL-4), IL-10, immune complexes, glucocorticoids and transforming growth factor β (TGF-β) (Murray *et al.* 2014). M1 macrophages are pro-inflammatory and play an important role in the defence against pathogens (Murray and Wynn 2011, Murray *et al.* 2014). M2 macrophages, on the other hand, promote tissue repair, cell proliferation and clearance of apoptotic cells and debris (Murray and Wynn 2011, Rőszer 2015).

Both M1 and M2 activated macrophages have been implicated in the pathogenesis of several diseases, including asthma and allergic disease (Murray and Wynn 2011). M2 macrophages in the lung are associated with asthma, although their exact contribution to the pathogenesis of the disease is currently unknown (Byers and Holtzman 2010, Sica and Mantovani 2012).

1.2.2 Asthma and allergy

Allergy is an immunological disorder in which an inappropriate immune response is initiated against an antigen (allergen) that normally poses no threat. Allergic disease can take many forms, depending on the individual, antigen and route of exposure, and the symptoms may be localized to a particular area or be systemic (Parham 2014). Allergic disease in the respiratory system may manifest as allergic rhinitis or allergic asthma (Parham 2014). Allergic asthma is primarily a T_H2-mediated disease and involves both resident and recruited immune cells, as well as the structural cells of the airways (Orihara *et al.* 2010). Exposure to the antigen leads to the release of inflammatory mediators into the extracellular environment, causing rapid vasodilation, smooth muscle contraction and a state of inflammation in the surrounding tissue (Orihara *et al.* 2010).

A range of factors seems to contribute to the development of allergic disease, including various genetic and environmental factors (ERS 2013). Atopic individuals have a genetic predisposition for developing allergic disease, stemming from polymorphisms in genes involved in the adaptive immunity (Parham 2014). With regard to environmental factors, certain substances may facilitate the process of sensitisation by acting as adjuvants. These substances typically act by enhancing the delivery of antigen, by stimulating the release of signals that promote the initiation of adaptive immune

responses or by engaging the innate immune system (Cox and Coulter 1997, Schijns 2003, Chalubinski and Kowalski 2006).

1.3 Phthalates

1.3.1 Properties and exposure

Phthalates are diesters of 1,2-benzenedicarboxylic acid (phthalic acid) and are primarily used as plasticizers in PVC products to increase their plasticity and longevity (Giam *et al.* 1984). Some of the most commonly encountered phthalates are di-n-butyl phthalate (DBP), dimethyl phthalate (DMP), diethyl phthalate (DEP), di-isobutyl phthalate (DiBP), butylbenzyl phthalate (BBzP), di (2-ethylhexyl) phthalate (DEHP), diisononyl phthalate (DiNP), diisodecyl phthalate (DiDP) and di (2-propylheptyl) phthalate (DPHP) (Wormuth *et al.* 2006, Wittassek and Angerer 2008). Phthalates are not covalently bound to the plastic polymers and may be released into the ambient environment through evaporation and abrasion (Fromme 2011). As a consequence, phthalates are among the most commonly encountered indoor contaminants (Wormuth *et al.* 2006).

DBP is a low molecular weight phthalate that is primarily used as a plasticizer in resins and PVC plastics. It is also used as a solvent for oil-soluble dyes, pesticides, peroxides and organic compounds, and as a softener in adhesives, printing inks, nitrocellulose paints, sealants, film coatings and glass fibres. It has been widely applied in cosmetics where it is used as perfume solvent and fixative, suspension agent for solids in aerosols, a lubricant for aerosol valves, an anti-foamer, a skin emollient and a plasticizer in nail polish (ECHA 2010). In addition, DBP is found in relatively high concentrations in certain medications and food supplements where it is used as a constituent of the enteric coating (Hauser *et al.* 2004, Hernandez-Diaz *et al.* 2009). DBP can also be a constituent of black tattoo inks (Lehner *et al.* 2011).

Because of the widespread and diverse use, exposure to DBP is considered to be ubiquitous. Several biomonitoring and screening studies have detected the metabolites of DBP in a high percentage of the study population, with some studies reporting the presence of metabolites in 97-99% of the test subjects (Silva *et al.* 2004, Wittassek *et al.* 2011, Frederiksen *et al.* 2014). The most important sources of exposure are ingestion of contaminated food, use and accidental ingestion of cosmetics and personal care

products, and inhalation of airborne particulate matter (Wormuth *et al.* 2006). DBP is among the phthalates found in the highest concentrations in indoor air and inhalation exposure has been estimated to account for up to 20% of total intake (Fromme *et al.* 2004, Otake *et al.* 2004, Bølling *et al.* 2013). Transdermal uptake of DBP directly from air is also a potential route of exposure (Weschler *et al.* 2015).

The half-life for DBP in the body is short and most of an applied dose is excreted in urine within 24 hours (Anderson *et al.* 2001, Seckin *et al.* 2009). DBP is also excreted via other pathways such as faeces and breast milk and sweat, but these are minor compared with the urinary pathway (Tanaka *et al.* 1978, Högberg *et al.* 2008, Genuis *et al.* 2012). The primary metabolite is the simple monoester mono-n-butyl phthalate (MBP), which is produced by hydrolysis catalysed by nonspecific lipases and esterases (Frederiksen *et al.* 2007). MBP accounts for approximately 64-84% of the total urinary metabolite load (Anderson *et al.* 2001, Seckin *et al.* 2009, Koch *et al.* 2012). Secondary metabolism by oxidation of the primary metabolite occurs, albeit at a lower rate than for heavier phthalates such as DEHP and DIHP (Frederiksen *et al.* 2007). The main oxidized metabolite is 3-OH-MBP, which accounts for approximately 7% of the total load. Other secondary metabolites are 2-OH-MBP, 4-OH-MBP and 3-carboxy-mono-propyl phthalate (MCCP), however these only make up a small fraction compared with MBP and 3-OH-MBP (Anderson *et al.* 2001).

1.3.2 Toxic effects of phthalates

The greatest concern regarding phthalate exposure, and thus the subject of most research, has been their endocrine disrupting properties and associated reproductive toxic effects. A recent review summarized a number of studies linking exposure to various phthalates to outcomes such as gestational age, body size measures, reproductive hormones, genital development, neurodevelopment, thyroid function, semen quality, precocious puberty and certain pregnancy complications (Jurewicz and Hanke 2011). As a consequence, the Commission of the European Union and the US Consumer Product Safety Commission has prohibited the manufacture, use and importation of toys and childcare articles containing concentrations of more than 0.1% of the phthalates DEHP, DiNP, DBP, BBzP, DiDP and di-n-octyl phthalate (DOP) (EU 2005, CPSC 2008). In the EU, DBP and DEHP is also banned from use in cosmetics (EU 2009).

In the last two decades, increasing evidence has emerged indicating that phthalate exposure can contribute to the development or exacerbation of allergic disease and reduced respiratory function (Jurewicz and Hanke 2011). Several epidemiological studies have shown an association between exposure to various phthalates and asthma, reduced pulmonary function, rhinitis, allergic sensitization and dermatitis, using urinary levels of metabolites and/or the concentrations of phthalates in dust as an indicator of exposure (Bornehag *et al.* 2004, Hoppin *et al.* 2004, Hsu *et al.* 2012, Bertelsen *et al.* 2013, Whyatt *et al.* 2014, Bekö *et al.* 2015, Franken *et al.* 2017). Moreover, several studies report correlations between the presence of different building materials in homes, acting as a proxy for phthalate exposure, and the incidence of allergic and airway disease and symptoms (Jaakkola *et al.* 2000, Jaakkola *et al.* 2004, Bornehag *et al.* 2005, Shu *et al.* 2014). Many of these materials can contain large amounts of phthalates, however, as they are not the sole constituents of these materials with toxic properties, these associations cannot be attributed to the phthalates alone.

With regard to DBP, specific associations have been reported between exposure and the incidence of respiratory symptoms and allergic disease. Franken *et al.* (2017) showed a significant association between the diagnosis of asthma and the urinary content of MBP and metabolites of DEHP in youths. In another study, a diagnosis of asthma, or having a history of asthma-like symptoms, was also associated with prenatal exposure to DBP, based on the urinary concentrations of MBP. Similar associations were observed for BBzP (Whyatt *et al.* 2014). Moreover, the urinary concentrations of MBP, as well as MEP, were associated with decrements in pulmonary parameters in adults (Hoppin *et al.* 2004). When assessing the impact of phthalate exposure through different measures of exposure (mass fractions of dust in homes and day-care, urinary content of metabolites and estimated daily indoor intakes), Bekö *et al.* (2015) found no association with asthma, rhinoconjuctivitis or atopic dermatitis. However, allergic sensitisation was significantly associated with exposure to DBP, BBzP and DEHP in children with the diseases. Specifically, allergic sensitisation was associated with indoor intake of DBP and BBzP, as well as the level of DEHP in home dust, but not with their metabolites in urine. Since the urinary metabolite levels reflect the total phthalate intake, this points towards the importance of non-dietary exposure routes such as inhalation or dermal absorption (Bekö *et al.* 2015).

In vivo and *in vitro* studies show that a range phthalates can exhibit immunomodulatory effects, including altered antibody expression and changes in cytokine and chemokine production (Kimber and Dearman 2010). However, no conclusive pattern has emerged and the effects are mostly found at doses and routes of exposure less relevant for the human population (Kimber and Dearman 2010). Nevertheless, some recent *in vivo* studies report adjuvant-like effects of orally administered DEHP on respiratory and allergy endpoints at concentrations relevant for human exposure (Guo *et al.* 2012, Han *et al.* 2014).

As previously stated, macrophages are central to the innate immunity and are implicated in the pathogenesis of asthma through release of inflammatory and chemotactic mediators and interactions with the adaptive immunity (Byers and Holtzman 2010, Murray and Wynn 2011). Several *in vitro* studies report immunomodulatory effects of DBP on macrophages and macrophage-like cells (Li *et al.* 2013, Couleau *et al.* 2015, Kim *et al.* 2015, Olderbø 2015, Teixeira *et al.* 2015, Steensen 2016). Although the results vary between experiments and model systems, DBP has been reported to alter the release of cytokines, reduce phagocytic activity, immunogenicity and antigen presenting capacity, and alter the expression of surface proteins involved in these functions, such as CD36, CD80 and major histocompatibility complex (MHC) class II molecules (Li *et al.* 2013, Couleau *et al.* 2015, Kim *et al.* 2015, Olderbø 2015, Teixeira *et al.* 2015, Steensen 2016).

A potential candidate for mediating the immunomodulatory effects of phthalates is peroxisome proliferator-activated receptor gamma (PPARγ), a nuclear receptor that is highly expressed in alveolar macrophages and has an anti-inflammatory role (Asada *et al.* 2004, Bølling *et al.* 2013). Activation of PPARγ has also been shown to prime human monocytes into M2 macrophages (Bouhlel *et al.* 2007), thus providing a possible link to the development or exacerbation of allergic disease.

1.4 PPARγ

Peroxisome proliferator-activated receptors (PPAR) are a family of ligand-activated transcription factors in the nuclear hormone receptor superfamily (Nuclear Receptors Nomenclature Committee 1999). There are three isotypes, PPARα, PPARβ/PPARδ and

PPARγ, which exhibit different functions and tissue distributions (Nuclear Receptors Nomenclature Committee 1999, Feige *et al.* 2006, Yessoufou and Wahli 2010).

PPARγ is predominantly expressed in adipose tissue, but is also found in smaller quantities in the large intestine, kidney, liver, small intestine, muscles, lungs and cells of the immune system (Fajas *et al.* 1997, Standiford *et al.* 2005). It regulates the expression of genes that are involved in lipid transport and storage, adipogenesis, cell division and differentiation and inflammation. PPARγ is an important regulator of inflammation and elicits anti-inflammatory responses when activated (Asada *et al.* 2004, Standiford *et al.* 2005, Becker *et al.* 2006). PPARγ regulates transcription by binding to peroxisome proliferator response elements (PPRE) in the regulatory region of genes as a heterodimer with retinoid X receptor (RXR). In the absence of a ligand, the heterodimer is associated with a number of co-repressors that supresses the transcriptional activity. Binding of a ligand induces dissociation with co-repressors and recruitment of co-activators resulting in transcription of the targeted gene (Feige *et al.* 2006, Kim *et al.* 2013).

The PPARγ ligand-binding domain (LBD) consists of 12 α-helixes and a β-sheet consisting of four strands (Figure 1A and 1B) (Uppenberg *et al.* 1998). Helixes 4, 5 and 8 are arranged between helixes 1, 3, 7 and 10 at the top of the LBD, forming the scaffolding for the ligand-binding site by anchoring helix 3, 7 and 10 (Nolte *et al.* 1998). The PPARγ ligand-binding site is located on the bottom half of the LBD and is formed by two interconnected cavities extending into a surface-accessible groove (Figure 1C) (Uppenberg *et al.* 1998). One cavity is made up of the side chains from helixes 3, 5, 10, 11 and 12, while the second cavity extends towards helix 1 and the β-sheet (Uppenberg *et al.* 1998). The canonical ligand-binding site is located in the cavity next to helix 12, while an alternative ligand-binding site has been identified in the area comprising the β-sheet, helix 2b and the Ω-loop (Figure 1C) (Hughes *et al.* 2014). The main ligand entry and exit point is postulated to be the groove delimited by helixes 1, 2 and 3, and the Ω-loop (Figure 1C) (Genest *et al.* 2008, Aci-Sèche *et al.* 2011).

PPARγ ligands include endogenous fatty acids and fatty acid derivatives as well as synthetic agonists in the thiazolidinedione (TZD) family (Krey *et al.* 1997). Synthetic full agonists, such as the TZD rosiglitazone, bind to the canonical ligand-binding site and stabilize helix 12 (Nolte *et al.* 1998, Bruning *et al.* 2007, Hughes *et al.* 2014).

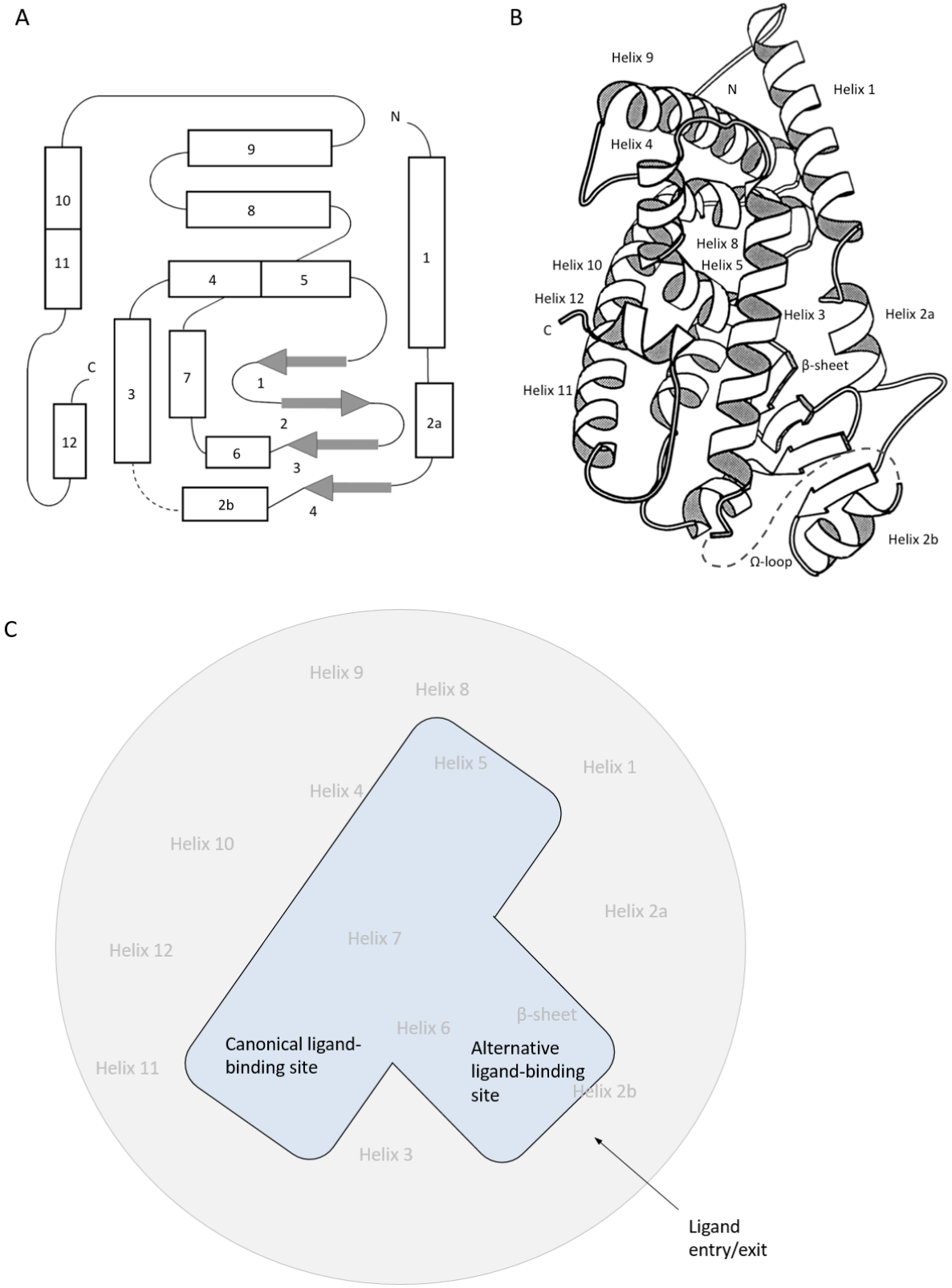

Figure 1. The *structure of the apo-PPARγ ligand-binding domain.* (A) Schematic diagram of the secondary structure of the apo-PPARg-LBD. Boxes and arrows represent α-helixes and β-strands, respectively. (B) Tertiary structure of the apo-PPARγ-LBD. Both A and B is adapted from Uppenberg *et al.* (1998). (C) A schematic illustration of the apo-PPARγ-LBD. The cavity and groove that forms the canonical and alternative ligand-binding sites are coloured blue, while the surrounding structures are coloured grey.

Synthetic partial agonists, offering graded transcriptional responses, interact less with helix 12 and instead stabilize residues in the alternative ligand-binding site (Bruning *et al.* 2007, Hughes *et al.* 2014). Endogenous fatty acid ligands may activate the receptor in a manner dependent or independent of helix 12 (Itoh *et al.* 2008, Waku *et al.* 2009). In addition, several endogenous ligands, like the eicosanoid 15-deoxy-$\Delta^{12,14}$-prostaglandin J_2 (15d-PGJ_2), bind covalently to the Cys285 residue of helix 3 (Shiraki *et al.* 2005, Itoh *et al.* 2008, Waku *et al.* 2009). Cys285 is also the target of synthetic PPARγ antagonists, such as GW9662 and T0070907, which block the binding of agonists to the canonical ligand-binding site (Hughes *et al.* 2014).

The PPARγ-LBD is larger and more accessible from the surface compared with the LBDs of other nuclear receptors, allowing it to accommodate many different ligands (Nolte *et al.* 1998, Uppenberg *et al.* 1998). In line with this, the binding of multiple ligands to the same LBD has been reported, both for two identical ligand molecules and for two molecules of different ligands (Itoh *et al.* 2008, Waku *et al.* 2010, Hughes *et al.* 2014). Moreover, certain ligands may shift between multiple binding configurations within the LBD, resulting in graded transcriptional responses (Hughes *et al.* 2012).

Several phthalates and their monoester metabolites, including DBP, have been reported to act as agonist for PPARγ (Hurst and Waxman 2003, Lampen *et al.* 2003, Feige *et al.* 2007, Kusu *et al.* 2008, Fang *et al.* 2015). However, phthalates show weaker agonistic activity compared to strong synthetic agonists (Kusu *et al.* 2008, Fang *et al.* 2015). Dysregulation of PPARγ and its anti-inflammatory properties may thereby provide a possible link to the respiratory effects of these chemicals (Bølling *et al.* 2013, Olderbø 2015). Moreover, the activation of macrophages by M2 stimuli is mediated by PPARγ and is dependent on signalling by the PPARγ-regulated cell-surface protein CD36 (Oh *et al.* 2012, Huang *et al.* 2014).

1.5 CD36

CD36, also known as fatty acid translocase (FAT) and SCARB3, is an integral membrane glycoprotein in scavenger receptor class B (Febbraio *et al.* 2001). Its expression is mainly regulated by PPARγ and occurs in a number of cell types including monocytes, macrophages, dendritic cells, erythrocytes, platelets, adipocytes, skeletal muscle cells and endothelial and epithelial cells of various tissues (Febbraio *et al.* 2001). Ligands for

CD36 include oxidized low-density lipoproteins (oxLDL), long-chained fatty acids (LCFA), oxidized phospholipids, components of bacterial cell walls, cell derived particles and apoptotic cells (Park 2014). CD36 plays an important role in the uptake of oxLDL and LCFA, angiogenesis, lipid metabolism and endocytosis of apoptotic cells by macrophages (Febbraio *et al.* 2001). In macrophages, the expression of cell-surface CD36 increases during monocyte to macrophage differentiation by increased expression and glycosylation of intracellular CD36 precursor (Alessio *et al.* 1996, Tontonoz *et al.* 1998).

2 Aims of the study

This master thesis is part of the project *Inhalation and prenatal exposure to phthalates: Influence on airway immunology*. The primary objective of the project is to evaluate effects of inhalation and prenatal exposure to phthalates on recruitment, activation and functionality of airway immune cells, as well as to identify possible biomarkers for airway effects of phthalates.

The aim of the present study was to clarify the mechanistic basis for the previously observed immunomodulatory effects of DBP during the PMA-induced differentiation of THP-1 cells into macrophage-like cells (Olderbø 2015), focusing on the expression of the surface marker CD36.

The main hypothesis was that the observed effects of DBP are mediated through interactions with the nuclear receptor PPARγ. To test this hypothesis, several working hypotheses were formulated and tested.

First, we hypothesised that the level of PMA-induced CD36 would be greater in cells exposed to known strong PPARγ agonists.

- The synthetic agonist rosiglitazone will enhance the PMA-induced levels of CD36, compared with control.
- The natural agonist 15-deoxy-$\Delta^{12,14}$-prostaglandin J_2 will enhance the PMA-induced levels of CD36, compared with control.

Second, we hypothesised that DBP would reduce the effects of strong PPARγ agonists.

- Exposure to DBP and the agonist in combination will reduce the PMA-induced expression of CD36, compared with cells exposed to the agonist alone.

Third, we hypothesised that a known PPARγ antagonist could block the effects of DBP.

- Exposure to GW9662 will not alter the level of PMA-induced CD36 by itself.
- Pre-incubation with GW9662, before exposure to DBP, will reduce the effects of DBP on the PMA-induced expression of CD36.

Fourth, we hypothesised that the effects on the CD36 levels occurred during, and not prior to the PMA-induced differentiation of the cells.

- Compared with controls, exposure to DBP, rosiglitazone or 15-deoxy-$\Delta^{12,14}$-prostaglandin J_2 will not increase the levels of CD36 in THP-1 monocytes.

Finally, we hypothesised that the activation of PPARγ would reflect the effects observed for the PMA-induced CD36 expression.

- Exposure to DBP, rosiglitazone, 15-deoxy-$\Delta^{12,14}$-prostaglandin J_2 and GW9662 will alter the amount of activated PPARγ in nuclear extracts in a manner analogous to their respective effects on CD36 expression.

3 Materials and methods

3.1 Reagents, chemicals and equipment

The reagents, chemicals and equipment applied in the experimental procedures are listed in Appendix 1.

3.2 Solutions and buffers

The solutions and buffers applied in the experimental procedures are listed in Appendix 2.

3.3 Cell line and exposure

3.3.1 THP-1

THP-1 is a human leukemic cell line cultured from the blood of a one-year-old boy with acute monocytic leukaemia (Tsuchiya *et al.* 1980). The cell line was chosen for this study because of its ability to differentiate into macrophage-like cells with characteristics of native monocyte-derived macrophages when exposed to PMA (Auwerx 1991), thus making them a commonly used model system for the resident pulmonary macrophages of the respiratory system (Daigneault *et al.* 2010). In addition, THP-1 cells have been shown to express CD36 under transcriptional regulation by PPARγ (Tontonoz *et al.* 1998).

Upon arrival, the THP-1 cells were cultured for two weeks before being frozen in aliquots in liquid nitrogen. Prior to the experiments, the cells were thawed at 37°C and mixed with cell culture medium containing 20% foetal bovine serum (FBS). For the first two weeks the cells were kept at a density of 6-8x10^5 cells/mL to reach the exponential growth phase, after which the cell cultures were maintained at approximately 5x10^5 cells/mL to ensure optimal growth. The concentration was maintained by splitting the cells every Monday, Wednesday and Friday. The concentration in each flask was determined using a LUNA II automated cell counter before a volume of cell suspension was taken out and mixed with pre-heated medium to reach the desired concentration

and volume. Each Monday the cell suspension was centrifuged for 5 minutes at 1000 rpm and the supernatant discarded. The pellet was then resuspended in medium and transferred to a new flask. The cell cultures were grown in 75 cm^2 cell culture flasks, suspended in approximately 20 mL medium, and incubated at 37°C in a Galaxy S+ incubator with an atmosphere containing 5% CO_2. All preparation and handling of the cells was performed in sterile conditions.

3.3.2 Exposure regimes

The effect of the experimental treatments on the differentiation of the cells, from monocytes to PMA-differentiated macrophages, and whether or not the effects were mediated through PPARγ was assessed using exposure regime I (Figure 2). Cells were seeded in 12 or 24 well cell culture plates to a density of $5x10^5$ cells/ml, in a volume of 1 mL or 0.5 mL, respectively. The cells were then given the experimental treatment and incubated at 37°C with an atmosphere containing 5% CO_2. After 24 hours, the cells were exposed to 50 ng/mL PMA and incubated for another 48 hours to differentiate them into macrophage-like cells. After a total of 72 hours, the cells were harvested for analysis. The 12 and 24 cell culture plates were used for preparing samples for flow cytometry analysis and for cell viability assays, respectively.

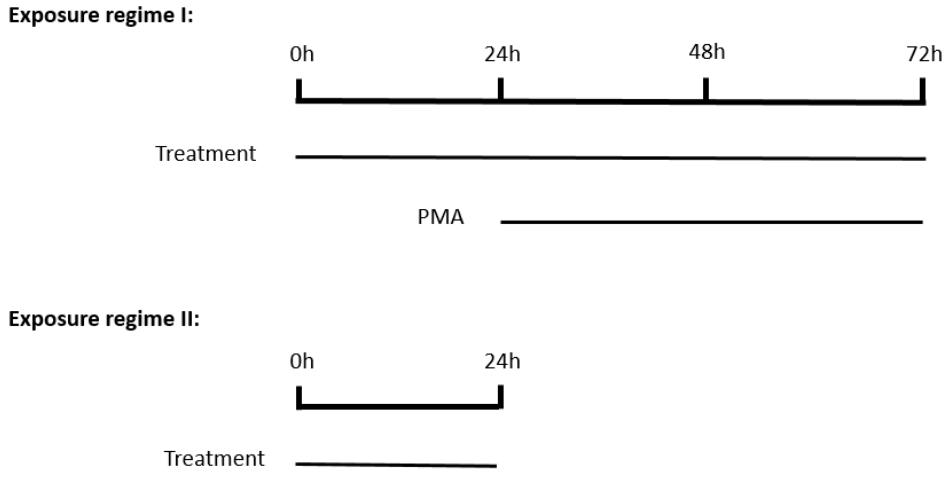

Figure 2. Exposure regimes. See main text section 3.3.2 for details.

Exposure regime II (Figure 2) was used to assess the effects on the expression of CD36 in undifferentiated THP-1 monocytes. Cells were seeded in 12 well cell culture plates to a density of $5x10^5$ cells/mL, in a volume of 1 mL. The cells were then exposed to the experimental treatment for 24 hours before being harvested for flow cytometry analysis.

3.3.3 Experimental treatments

Cells were treated with 20, 40 or 80 µM DBP to assess its ability to influence the expression of CD36 during differentiation of THP-1 monocytes into macrophage-like cells (Table 1). The concentrations chosen for this study were derived from estimates of pulmonary exposure to DBP, based on indoor air levels and the volume of inhaled air, assuming total absorption of the phthalate in the lung (Bølling *et al.* 2013), and have previously been shown to affect the chosen endpoint in the applied model system (Olderbø 2015).

The involvement of PPARγ was assessed by exposing the cells to the PPARγ agonists rosiglitazone and 15d-PGJ_2, and the PPARγ antagonist GW9662, either alone or in combination with DBP (Table 1). In pilot studies 80 µM DBP showed the most pronounced effects on CD36 expression and was thus chosen for the combinatory treatments. Both rosiglitazone and 15d-PGJ_2 are potent PPARγ agonists and interacts with the canonical ligand-binding site in a non-covalent and covalent manner, respectively (Shiraki *et al.* 2005, Bruning *et al.* 2007). The antagonist GW9662 binds covalently to the same residue as 15d-PGJ_2, thereby efficiently blocking the PPARγ-LBD (Leesnitzer *et al.* 2002). The concentrations of rosiglitazone (0.005, 0.05 and 0.5 µM), GW9662 (0.1, 1 and 10 µM) and 15d-PGJ_2 (0.1, 0.5 and 1 µM) were chosen based on pilot studies and concentrations reported in literature (data not shown).

Stock solutions of DBP, rosiglitazone, GW9662 and 15d-PGJ_2 were prepared and diluted in dimethyl sulfoxide (DMSO) so that a volume could be added to the wells, corresponding to a 1:1000 or 1:500 dilution per ml medium, yielding the final concentrations (Table 1). The total concentration of DMSO in each well was kept equal between all wells and below 0.5% of the total volume.

Table 1. Experimental treatments.

Treatment	Stock concentration (mM)	Concentration in well (µM)
Di-n-butyl phthalate	10[1], 20[1], 40[1]	20, 40, 80
Rosiglitazone	0.005[2,3], 0.05[2,3], 0.5[1,3]	0.005[3], 0.05[3], 0.5[3]
GW9662	0.1[2,3,4], 1[2,3], 10[1,3]	0.1[3,4], 1[3], 10[3]
15-deoxy-$\Delta^{12,14}$-Prostaglandin J_2	0.1[2], 0.5[2], 1[2], 5[1,3]	0.1[3], 0.5[3], 1[3], 5[3,4] , 10[3,4]

[1] Main stock.
[2] Diluted from main stock.
[3] Concentration was used in combinatory treatment with 80 µM DBP.
[4] Concentration was tested in pilot experiments.

3.4 Analysis of cell-surface CD36 using flow cytometry

Flow cytometry is an analytical method in which the physical and chemical parameters of individual particles in a sample are analysed using scattered light and fluorescent labelling (Figure 3). In the present study, the method was applied for analysing cells in suspension. The sample is injected into the flow cell of the flow cytometer, which contains a stream of liquid called the sheet fluid (Figure 3 (i)). The sheet fluid is driven through the flow cell by air pressure and focuses the sample stream so that the particles are carried to the point of measurement in single file (Figure 3 (ii)). At this point the sample flows through a light source and is illuminated (Figure 3 (iii)). The majority of instruments today uses lasers as light sources as these produce a focused beam of high intensity monochromatic light, which provides maximum excitation and reduces the probability of more than one particle being measured at a time. An optical system consisting of various lenses and filters focuses the light at the sample and directs the scattered light and the emitted fluorescent signal towards the appropriate detectors (Figure 3 (iv)). The analogue measurements from the detectors are then digitized and transferred to a workstation computer for further processing and analysis (Figure 3 (v)) (Ormerod 2008).

The flow cytometer measures light scatter at different angles as well as the emitted signal from fluorescent labels attached to the particle. Scattered light is divided into forward-scattered light, which reflects the size of the particle, and side-scattered light, which reflects its granularity and complexity. Fluorescent labels are commonly used to

provide additional information of the sample. These labels typically consist of a fluorochrome attached to an antibody with affinity for a particular structure of interest (Ormerod 2008).

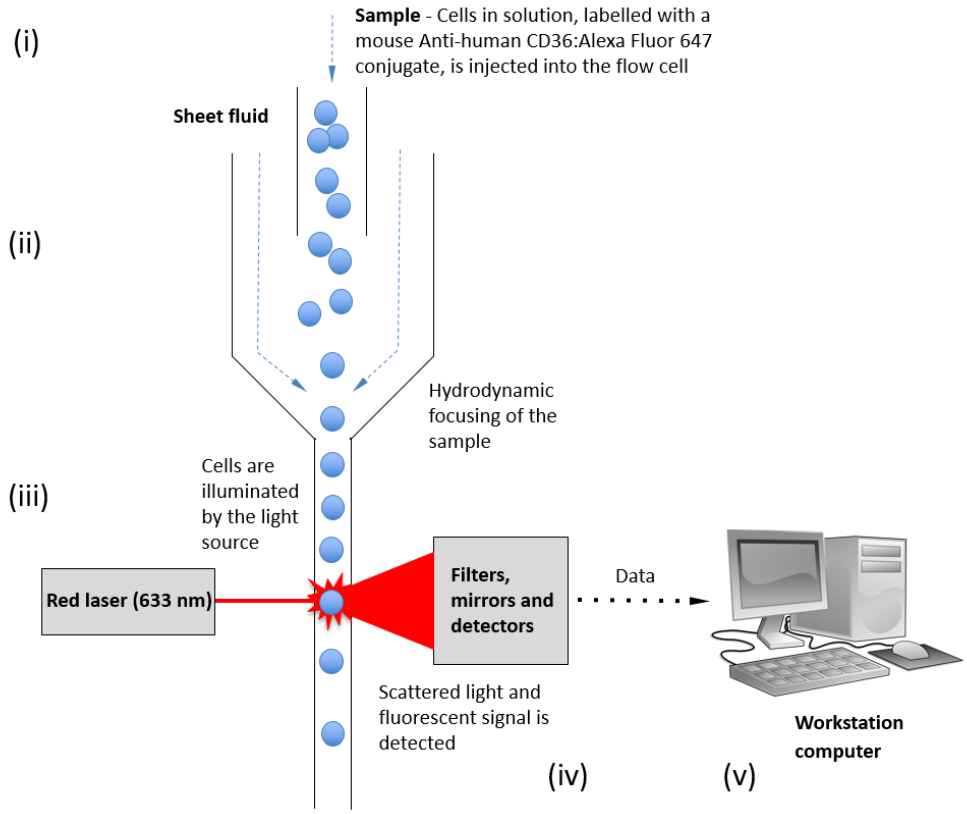

Figure 3. The main components and processes of flow cytometry analysis. See the main text for a more detailed description of the steps (i) to (v). Adapted from Ormerod (2008).

Prior to flow cytometry analysis, cells that were differentiated into macrophage-like cells were harvested using accutase, a cell detachment solution. The wells were first washed two times using 1 mL sterile Dulbecco's phosphate-buffered saline (PBS) to remove the medium and non-adherent cells. The PBS was then removed and 500 µL accutase added. Both the PBS and the accutase were equilibrated to room temperature before use. The plates were incubated for 3 minutes at 37°C before being knocked at the side of a table in order to detach the cells from the wells. This process was repeated three times, resulting in a total incubation time of 9 minutes. Following the final incubation, the plate was put on ice and the cell suspension was transferred to 1.5 mL eppendorf tubes before 1 mL sterile PBS was added to each well. Any remaining cells were loosened by repeatedly pipetting the PBS in the well before transferring the

suspension to the correct tube. For cells that were harvested for analysis before the PMA-induced differentiation the accutase treatment was not necessary, and the cells were simply transferred to the eppendorf tubes at the end of the exposure.

The harvested cells were stained with an anti-CD36 antibody conjugated with a fluorescent dye (Alexa Fluor 647) for flow cytometry analysis. Before staining was performed, the cells were washed twice using 1 mL flow cytometry staining buffer (FSB). In each washing step, the samples were centrifuged at 1200 rpm for 5 minutes and the supernatant discarded before the pellet was resuspended in FSB. Following the final washing step, the sample was centrifuged once more and the supernatant was removed before 50 µL blocking solution, consisting of 4% Human TrueStain FcX and 96% FSB, was added. The samples were then incubated on ice for 15 minutes during gentle shaking, after which 10 µL antibody solution was added to each tube and the incubation continued for another 30 minutes. Following the staining, the samples underwent three washing steps, as described above, in order to remove excess blocking solution and antibody. After the final centrifugation, as much of the supernatant as possible was removed before the pellet was resuspended in 350 µL FSB. The samples were transferred to 5 mL falcon tubes and analysed immediately using the BD LSR II flow cytometer. The cells were gated based on forward scattered and side scattered light to exclude debris and doublets (Figure 4A). Alexa Fluor 647, representing the expression

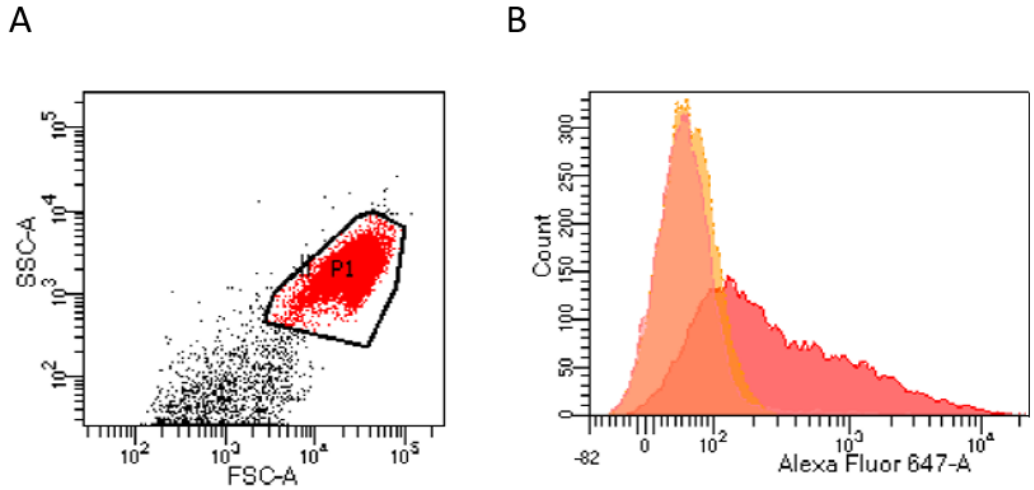

Figure 4. Example of gated cells and detected Alexa Fluor 647-A in a cell suspension. (A) To exclude doublets and debris, the cell samples were gated according to criteria represented by the black line. Red dots represent cells included in the subsequent analysis, while black dots represent cells excluded by the gating. (B) The level of Alexa Fluor 647-A, representing the expression of CD36, was analysed in the cell samples. The orange histogram represents undifferentiated monocytes, while the red histogram represents cells that had undergone PMA-induced differentiation. The yellow histogram represents PMA-treated cells that have not been stained with an antibody.

of CD36 on the cells, was detected using the red laser (633 nm) and a 660/20 filter (Figure 4B). A total of 10000 events were recorded for each treatment. The expression of CD36 is presented as the median fluorescence intensity of each treatment.

3.5 Cytotoxicity and cell viability assays

Cytotoxicity and cell viability was measured using the Cytotoxicity Detection kit^{PLUS} and the alamarBlue® cell viability assay, according to the manufacturers instructions. Samples for both assays were seeded on the same 24 well cell culture plate and exposed according to exposure regime I. The supernatant was harvested for assessment of cytotoxicity while the cells remaining in the wells were used for the cell viability assay.

3.5.1 Cytotoxicity

Cytotoxicity was calculated based on measurements of lactate dehydrogenase (LDH) activity in the cell culture supernatant. LDH is a cytoplasmic enzyme that is found in nearly all cells and is released when the cell is damaged or lysed. LDH enzyme activity in a cell-free supernatant thereby correlates with the amount of dead or damaged cells in the culture. A reaction mixture containing diaphorase/NAD+ mixture, INT and sodium lactate is added to the supernatant. LDH activity is measured by an enzymatic reaction in which 2-(4-iodophenyl)-3-(4-nitrophenyl)-5-phenyl-2*H*-tetrazolium (INT), a tetrazolium salt in the dye solution, is converted into red formazan dye. The dye can then be quantified by measuring absorbance at 490-500 nm (Roche).

After exposure, the supernatant samples harvested for LDH analysis was transferred to 1.5 mL eppendorf tubes. Selected wells were treated with 5 µL of Tritan-x-100, a cell-lysing agent, to serve as the LDH max control. The samples were then centrifuged at 1200 rpm for 5 minutes and the supernatant transferred to 96 well microtest storage plates. Awaiting analysis, the plates were sealed using an adhesive cover and stored at -80°C.

Prior to analysis the samples were thawed in room temperature. A standard curve was prepared by diluting a LDH concentrate solution (9259 U/mL) in medium. The concentrate was first diluted twice to form a primary stock of 1000 mU/mL. The primary stock was then series diluted to form the final standard curve concentrations

250 mU/mL, 125 mU/mL, 62.5 mU/mL, 31.2 mU/mL, 15.6 mU/mL, 7.8 mU/mL, 3.9 mU/mL and 0mU/mL. The LDH max control was diluted in medium in a 1:2 and 1:4 ratio to make sure the absorbance values would fit within the standard curve. Samples, diluted and undiluted LDH max control, and standards were then added to the wells of a 96 well maxisorb plate at a volume of 50 µL. To start the colour reaction, 50 µL of reaction mixture, consisting of approximately 2% catalyst (diaphorase/NAD+ mixture) and 98% dye solution (INT and sodium lactate), was added to each well before the plate was incubated at room temperature for 30 minutes in darkness. Absorbance was measured at 490 nm using a Sunrise remote microplate reader. Cytotoxicity in each sample was calculated as the amount of LDH in the sample (mU/mL) and as a percentage of the LDH max control.

3.5.2 Cell viability

AlamarBlue is a quantitative cell viability assay using fluorescence as an indicator of the metabolic activity of the cell sample. The active ingredient is resazurin, which is reduced to the fluorescent molecule resorufin upon entering a cell. Viable cells will continuously convert resazurin providing a quantitative measure of cell viability (ThermoFisher).

After the supernatant was harvested for LDH analysis, 450 µL of pre-heated medium was added to each well of the cell culture plate. Then, 50 µL of alamarBlue solution was added to each well to start the reaction, before the cell culture plate was incubated at 37°C in an atmosphere with 5% CO_2. Fluorescence was detected at 600 nm using a CLARIOstar plate reader after 30 minutes. Additional readings were performed at the 60 minutes, 90 minutes and 120 minutes mark, during which the plates were incubated in the plate reader at 37°C. Fluorescence from wells without cells were used to subtract the background levels from wells given the experimental treatments. The 60-minute mark was chosen for further analysis of cell viability (See Appendix 3).

3.6 PPARγ activation

To assess the state of PPARγ activation after exposure to the experimental treatments, nuclear extracts were analysed using a PPARγ transcription factor assay kit. The nuclear extracts were prepared using a nuclear extraction kit and evaluated using western

blotting. Several exposure regimes and experimental treatments were tested to establish the assay. However, due issues with the provided kits no viable data was produced. For full description of the PPARγ activation assay and the preparation of the nuclear extracts, see Appendix section 4.1 and 4.2.

3.7 Statistics

3.7.1 Normalization

Prior to statistical analysis, all values were adjusted through a two-step normalization procedure. First, each value in an experiment was divided by the mean value of all values in that particular experiment to even out the differences between experiments. Then, each value was divided by the mean of all the controls from all experiments and multiplied by 100. As a result, the values from the different experiments were scaled to the same level while still retaining variation in the control groups.

3.7.2 Statistical analysis

All statistical analysis was performed using the Graphpad Prism 5 software for Windows. Depending on the number of explanatory variables in the experimental design, the data sets were analysed using either 1-way ANOVA or 2-way ANOVA, with a Dunnets or Bonferroni post-test, respectively. P-values at or below 0.05 were considered statistically significant.

4 Results

4.1 Effects on the expression of cell-surface CD36

4.1.1 Di-n-butyl phthalate

To confirm that DBP upregulated CD36 in the applied model system, the cells were exposed to 20, 40 or 80 μM for 24 hours before being differentiated into macrophage-like cells using PMA (Exposure regime I). The level of cell-surface CD36 was determined using flow cytometry after a total exposure time of 72 hours. Cells treated with 80 μM DBP exhibited a statistically significant increase in CD36 expression when compared to control, corresponding to an average increase of approximately 19% (Figure 5). In contrast, treatment with 20 and 40 μM of DBP did not change the CD36 levels significantly.

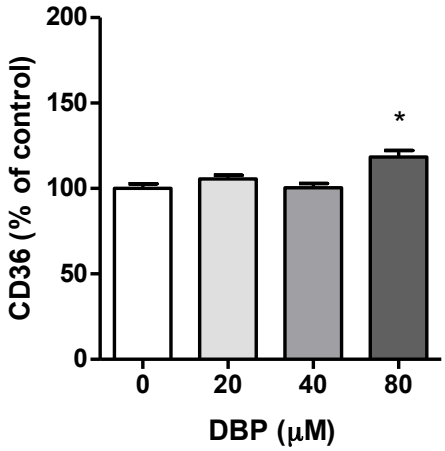

Figure 5. Expression of the surface marker CD36 on PMA-differentiated THP-1 cells after DBP exposure. THP-1 cells were exposed to 20, 40 or 80 μM of DBP for 24 hours, followed by 48 hours of PMA treatment, leading to a total exposure of 72 hours (exposure regime I). The level of CD36 expression, determined by flow cytometry, is represented as median fluorescence intensity (mean ± SEM). All values are normalized according to the two-step process described in section 3.7.1. Statistically significant ($p<0.05$) difference from control is indicated with an asterisk (*), based on a 1-way ANOVA with Dunnett's post-test (n=8 independent experiments).

4.1.2 Rosiglitazone

To examine whether CD36 was regulated by PPARγ in the applied cellular system, the cells were exposed to the known PPARγ agonist rosiglitazone (0.005 - 0.5 μM) (Exposure regime I). Cells exposed to rosiglitazone exhibited a concentration-dependent increase in CD36 expression compared with controls (Figure 6). Exposure to 0.05 and 0.5 μM rosiglitazone caused a statistically significant increase of 210% and 440%, respectively, while the lowest concentration of 0.05 μM caused a non-significant increase of 30%.

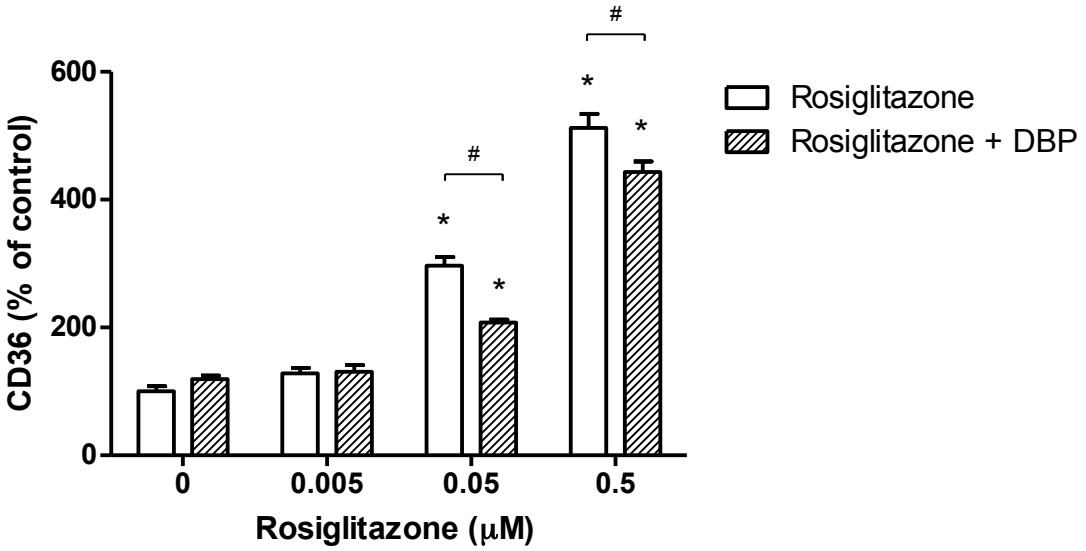

Figure 6. Expression of CD36 on PMA-differentiated THP-1 cells after exposure to rosiglitazone and DBP. The cells were exposed to 0.005, 0.05 and 0.5 μM rosiglitazone for 24 hours, either alone or in combination with 80 μM DBP, followed by 48 hour PMA treatment (Exposure regime I). The level of CD36 expression, determined by flow cytometry, is represented as median fluorescence intensity (mean ± SEM). All values are normalized according to the two-step process described in section 3.7.1. Statistically significant ($p<0.05$) difference between treatments is based on a 2-way ANOVA, with Bonferroni post-test (n=6 independent experiments). *: Rosiglitazone or rosiglitazone + DBP vs. respective control; #: rosiglitazone vs. rosiglitazone + DBP within the same concentration of rosiglitazone.

To asses if the effect of DBP could disturb the effects of a known PPARγ agonist binding reversibly to the canonical ligand-binding site, cells were exposed to the same concentrations of rosiglitazone in combination with 80 μM DBP. The combined treatment of 0.05 or 0.5 μM rosiglitazone with DBP lead to significantly lower levels of CD36 expression compared to cells exposed to rosiglitazone alone (Figure 6).

In line with the data presented in Figure 5, exposure to 80 µM DBP alone lead to an average increase in CD36 expression of 22% when compared to control. However, the increase was not statistically significant in this dataset (Figure 6).

4.1.3 GW9662

To assess whether or not a PPARγ antagonist could block the DBP-induced increase in CD36 expression, the cells were pre-incubated with 1 or 10 µM of GW9662 for 30 minutes before the 24-hour exposure to 80 µM DBP and subsequent PMA-induced differentiation (Exposure regime I). Exposure of cells to the antagonist GW9662 alone did not change the expression of CD36 significantly (Figure 7).

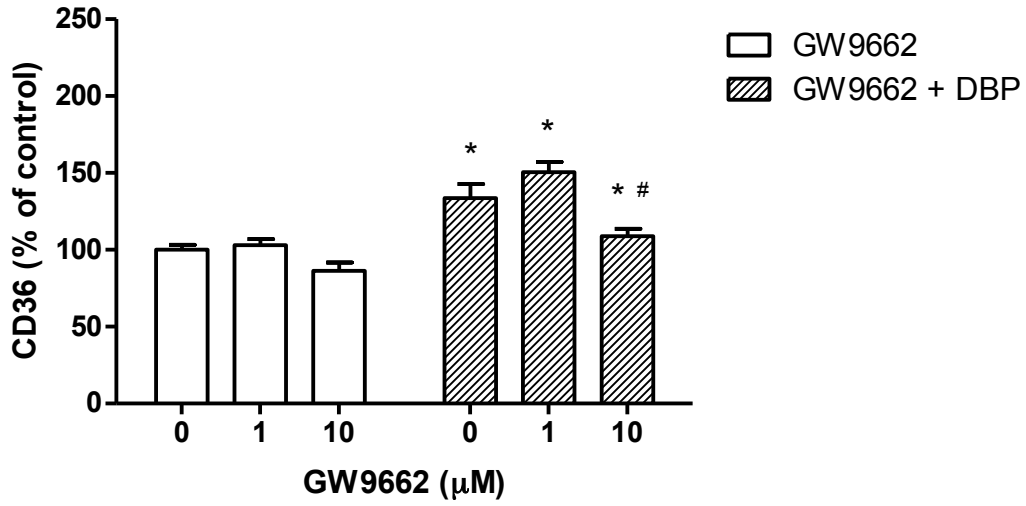

Figure 7. Expression of CD36 on PMA-differentiated THP-1 cell after exposure to the antagonist GW9662 and DBP. The cells were exposed to 1 and 10 µM GW9662 for 24 hours, either alone or in combination with 80 µM DBP, followed by 48 hours of PMA treatment (Exposure regime I). The level of CD36 expression, determined by flow cytometry, is represented as median fluorescence intensity (mean ± SEM). All values are normalized according to the two-step process described in section 3.7.1. Statistically significant ($p<0.05$) difference between treatments is based on a 2-way ANOVA with Bonferroni post-test (n=5 independent experiments). *: GW9662 vs. GW9662 + DBP within the same concentration of GW9662; #: GW9662 or GW9662 + DBP vs. respective control.

Pre-incubation with 10 µM of the antagonist significantly reduced expression of cell-surface CD36 induced by DBP, almost to the control level (Figure 7). In contrast, 1 µM of GW9662 tended to increase the CD36 expression induced by DBP, although not significantly (Figure 7). Furthermore, the effect of DBP in the presence of the antagonist was significantly higher than controls treated with the antagonist alone, for all concentrations tested (Figure 7).

In this set of experiments, exposure to 80 μM DBP alone induced a greater increase in CD36 expression compared to the data reported in Figure 5 and Figure 6. The effect was statistically significant and corresponded to a 35% increase in CD36 expression compared with control (Figure 7).

4.1.4 Rosiglitazone and GW9662

To assess the ability of GW9662 to effectively block effects mediated by activation of PPARγ, the effect of the antagonist was tested for 0.05 μM rosiglitazone. The concentration of rosiglitazone was chosen because it was the lowest dose exhibiting a statistically significant increase (Figure 6) and thus presumed to be the easiest to block. In line with the data presented in Figure 7, none of the GW9662 concentrations tested induced a significant change in CD36 expression (Figure 8). Pre-incubation with 0.1, 1, 5 and 10 μM GW9662 lead to a dose-dependent decrease in the effect of rosiglitazone, with 1 μM GW9662 being sufficient to block most of the effect of rosiglitazone and 5 μM enough to block it completely (Figure 8).

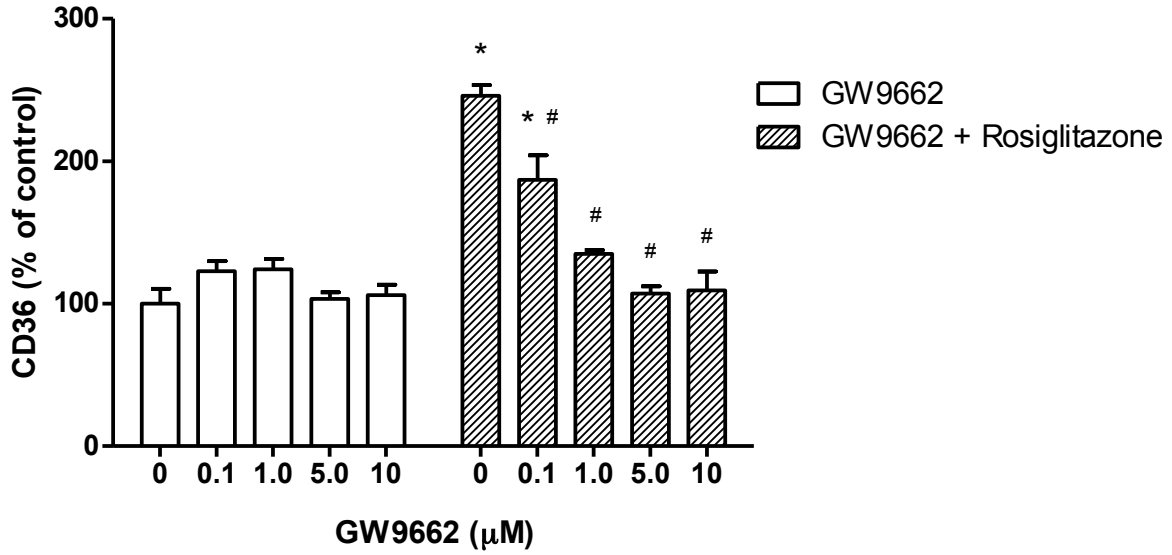

Figure 8. CD36 expression on PMA-differentiated THP-1 cell after exposure to GW9662 and rosiglitazone. The cells were exposed to 0.1, 1, 5 and 10 μM GW9662 for 24 hours, either alone or in combination with 0.05 μM rosiglitazone, before 48 hours of PMA treatment (Exposure regime I). The level of CD36 expression, determined by flow cytometry, is represented as median fluorescence intensity (mean ± SEM). All values are normalized according to the two-step process described in section 3.7.1. Statistically significant ($p<0.05$) difference between treatments is based on a 2-way ANOVA with Bonferroni post-test (n=3 independent experiments). *: GW9662 vs. GW9662 + rosiglitazone, within the same concentration of GW9662; #: GW9662 or GW9662 + rosiglitazone vs. respective control.

As indicated in Figure 7, DBP was not blocked by 1 μM GW9662. Since 1 μM was sufficient to block the rosiglitazone-induced effects, the decrease in DBP-induced CD36 expression observed at 10 μM GW9662 was likely due to non-specific binding of the antagonist. Consequently, the concentration of 1 μM GW9662 must be considered the effective concentration in this model system.

4.1.5 15-deoxy-$\Delta^{12,14}$-prostaglandin J_2

To further assess the interaction of DBP with PPARγ, cells were exposed to the natural ligand 15d-PGJ_2, which binds covalently to the PPARγ-LBD (Exposure regime I). Exposure to 0.1, 0.5 and 1 μM 15d-PGJ_2 lead to a dose-dependent increase in CD36 expressed on the cells (Figure 9), indicating that 15d-PGJ_2 can function as an agonist in the applied cellular system. Compared with control, the increase was statistically significant for all doses tested (Figure 9).

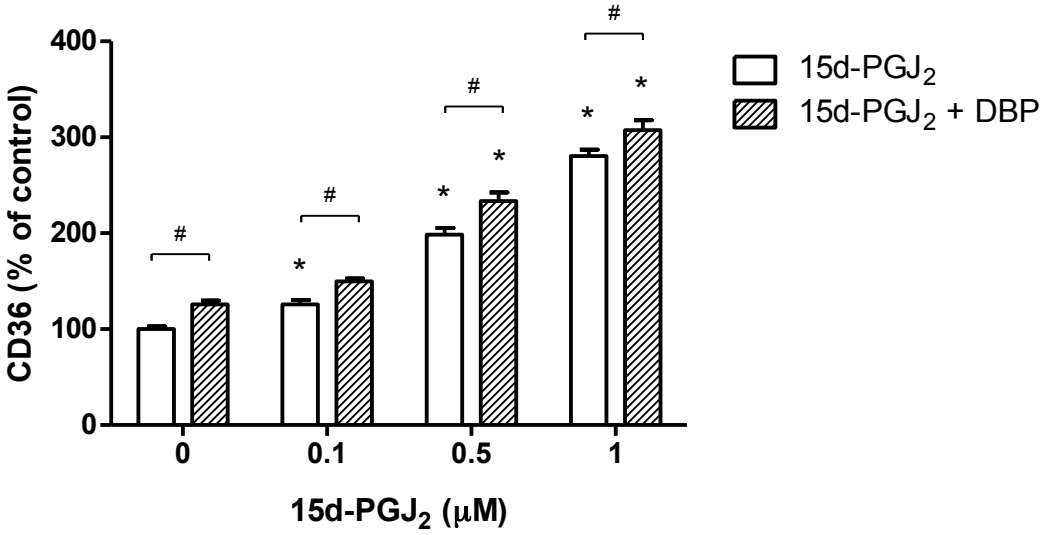

Figure 9. CD36 expression on PMA-differentiated THP-1 cells after exposure to 15d-PGJ_2 and DBP. The cells were exposed to 0.1, 0.5 and 1 μM 15d-PGJ_2 for 24 hours, either alone or in combination with 80 μM DBP, before 48 hours of PMA treatment (Exposure regime I). The level of CD36 expression, determined by flow cytometry, is represented as median fluorescence intensity (mean ± SEM). All values are normalized according to the two-step process described in section 3.7.1. Statistically significant ($p<0.05$) difference between treatments is based on a 2-way ANOVA with Bonferroni post-test (n=6 independent experiments). *: 15d-PGJ_2 or 15d-PGJ_2 + DBP vs. respective control; #: 15d-PGJ_2 vs. 15d-PGJ_2 + DBP, within the same concentration of 15d-PGJ_2.

For all concentrations of 15d-PGJ_2, combined exposure with 80 μM DBP lead to a statistically significant increase in CD36 expression compared to cells exposed to only

15d-PGJ_2 (Figure 9). The numerical difference in CD36 expression was relatively stable for all concentrations (25-35%), pointing towards an additive effect.

4.1.6 CD36 expression in THP-1 monocytes

To determine whether the increased CD36 expression occurred prior to, or during the PMA-induced differentiation, THP-1 monocytes were exposed to either 80 μM DBP, 0.5 μM rosiglitazone or 5 μM 15d-PGJ_2 (Exposure regime II). None of the concentrations tested exhibited any statistically significant change when compared to control (Figure 10).

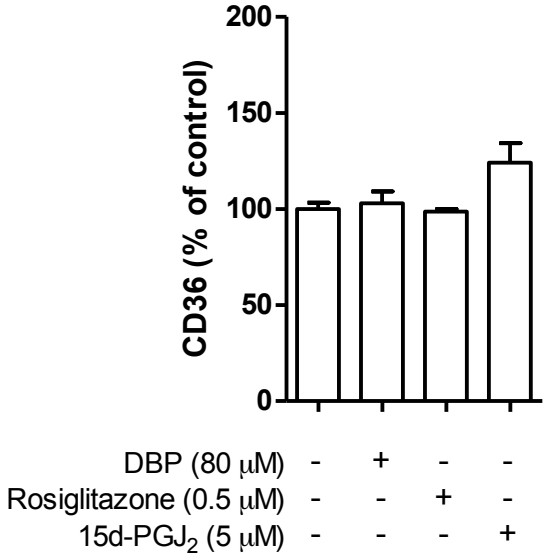

Figure 10. CD36 expression in undifferentiated THP-1 cells after exposure to DBP, rosiglitazone and 15d-PGJ_2. Cell were exposed to either 80 μM DBP, 0.5 μM rosiglitazone or 5 μM 15d-PGJ_2 for 24 hours (Exposure regime II). The expression of CD36 was determined using flow cytometry. Values are represented as median fluorescence intensity (mean ± SEM). All values are normalized according to the two-step process described in section 3.7.1. Statistical significance ($p<0.05$) is based on a 1-way ANOVA (n=3 independent experiments).

4.2 PPARγ activation

Neither rosiglitazone nor 15d-PGJ_2 appeared to activate PPARγ to a greater extent than controls in nuclear extracts after 3 hours or 24 hours exposure (Exposure regime II). Addition of PMA for the last 3, 24 or 48 hours (Exposure regime I) did not alter this outcome. Due to inability to detect activated PPARγ using rosiglitazone and 15d-PGJ_2, the activation of PPARγ by DBP was not assessed. For the results of the nuclear extraction procedure and the PPARγ activation assay, see appendix section 4.3.

4.3 Cell viability and cytotoxicity

To examine if the effects on CD36 expression described above were influenced by reduced cell viability or increased cytotoxicity, the metabolic activity of the cells and the level of LDH activity in the supernatant were measured after exposure to the highest concentrations of rosiglitazone (0.5 μM), GW9662 (10 μM), DBP (80 μM) and 15d-PGJ_2 (1 μM and 10 μM), both alone and in combination (Figure 11).

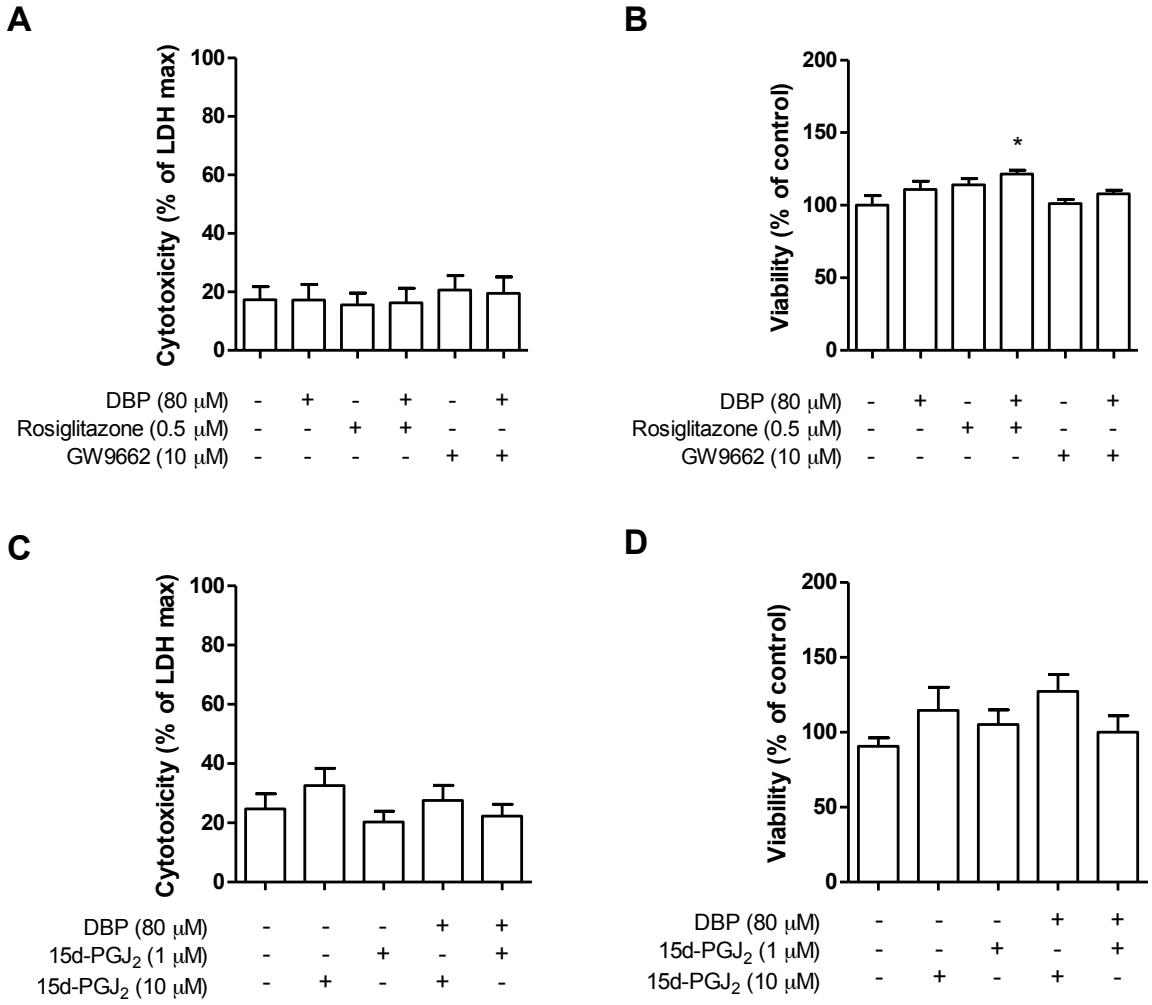

Figure 11. Cytotoxicity and cell viability after exposure to rosiglitazone, GW9662, 15d-PGJ_2 and DBP. THP-1 cells were exposed to rosiglitazone (0.5 μM), GW9662 (10 μM), DBP (80 μM) and 15d-PGJ_2 (1 μM and 10 μM) for 24 hours, either alone or in combination, prior to 48 hours of exposure to PMA (Exposure regime I). (A and C) Cytotoxicity is indicated by LDH activity in the supernatant, and calculated as a percentage of the LDH max control. (B and D) The metabolic activity of the cell samples was determined by the reduction of resazurin dye (alamarBlue assay). B and D values were normalized according to the two-step process described in section 3.7.1. Statistically significant ($p<0.05$) difference between treatments are indicated with an asterisk (*), based on a 1-way ANOVA with Dunnett's post-test (n=4 (A and B), n=3 (C) and n=2 (D) independent experiments).

None of the treatments tested caused a significant increase in cytotoxicity when compared to controls (Figure 11 A and C). Similarly, none of the treatments tested caused a decrease in metabolic activity (Figure 11 B and D). However, a combined exposure of DBP and rosiglitazone showed a statistically significant increase in fluorescence intensity of approximately 17% (Figure 11B).

5 Discussion

Exposure to environmental contaminants is suggested to be a contributing factor to the increased prevalence of asthma and allergic disease (Asher *et al.* 2006, Chalubinski and Kowalski 2006, Croisant 2014). DBP has been linked to allergic and respiratory symptoms in epidemiological studies (Hoppin *et al.* 2004, Whyatt *et al.* 2014, Bekö *et al.* 2015, Franken *et al.* 2017), and has been reported to affect immunological parameters in macrophages *in vitro* (Li *et al.* 2013, Couleau *et al.* 2015, Olderbø 2015, Teixeira *et al.* 2015). Although the intracellular signalling pathways responsible for mediating these effects are currently unknown, the nuclear receptor PPARγ is a potential candidate (Bølling *et al.* 2013).

In this study, the effect of DBP on the PMA-induced differentiation of THP-1 cells was investigated, focusing on the expression of the cell surface marker CD36. In addition, the involvement of PPARγ in mediating this effect was examined by combined exposure of DBP and the known PPARγ agonists rosiglitazone and 15d-PGJ_2, and the effects of the PPARγ antagonist GW9662. Both DBP and the PPARγ agonists enhanced the expression of CD36 during the PMA-induced differentiation, although the effect was much lower for DBP. Exposure to the reversibly binding agonist rosiglitazone in combination with DBP led to a reduction in cell-surface CD36 compared to cells exposed to rosiglitazone alone. In contrast, exposure to the covalently binding agonist 15d-PGJ_2 in combination with DBP appeared to cause an additive effect on the expression of CD36. Although dissimilar, both results indicate that DBP may interfere with PPARγ-mediated effects depending on the mode of interaction between the agonist and the PPARγ-LBD. The PPARγ antagonist GW9662 was shown to effectively block the effect of rosiglitazone, while the effective concentration did not inhibit the DBP-induced effect on CD36. Moreover, DBP significantly increased the CD36 expression in the presence of the antagonist.

5.1 DBP increases the expression of cell-surface CD36

In this study, exposure to 80 µM DBP enhanced the PMA-induced CD36 expression in THP-1 macrophages. The effect was relatively consistent throughout all sets of experiments, increasing the level of cell-surface CD36 by 19-35% (Figure 5, 6, 7 and 9). Using the same model system and concentrations as applied in the present study,

Olderbø (2015) detected a concentration-dependent increase in the levels of CD36 after exposure to DBP. However, the effect was greater and evident at lower concentrations compared with the results presented in this study. Exposure to DBP caused a significant increase at 40 µM, culminating to an increase of approximately 60% at 80 µM (Olderbø 2015). Conversely, Li *et al.* (2013) found that exposing mouse peritoneal exudate macrophages to DBP decreased the expression of CD36. The experimental model used in the current study was used to examine the effect of DBP on the differentiation of monocytes to macrophages, while Li *et al.* (2013) studied the effects of DBP on mature primary macrophages. Consequently, differences in the model systems may have contributed to the discrepancy between the observations. A number of differences have been reported between primary cells and immortalized cells lines, as well as between PMA-induced THP-1 macrophages and macrophages derived from primary human monocytes (Kohro *et al.* 2004, Pan *et al.* 2009, Daigneault *et al.* 2010). Furthermore, the macrophages used by Li *et al.* (2013) were extracted from mice, while the THP-1 cell line is of human origin, suggesting that species differences may be contributing to the disparity.

CD36 is a class B scavenger receptor involved in the uptake of oxLDL, fatty acids and modified phospholipids, as well as in the phagocytosis of bacteria, apoptotic cells and cellular debris (Febbraio *et al.* 2001, Park 2014). In macrophages, the level of CD36 is associated with phagocytic capacity (Fadok *et al.* 1998, Li *et al.* 2013, Woo *et al.* 2016). Phagocytosis is central to macrophage function in tissue homeostasis and host defence through removal of pathogens, dead cells, debris and foreign material (Murray and Wynn 2011). Thus, the higher levels of cell-surface CD36 induced by DBP may potentially alter macrophage function through increased phagocytosis. However, DBP reduced the phagocytic capacity in both mouse primary macrophages (Li *et al.* 2013) and LPS-stimulated THP-1 cells (Couleau *et al.* 2015). Moreover, previous experiments using the model system of the present study were unable to detect any effect of DBP on phagocytosis (unpublished data). Thus, the ability of DBP to influence phagocytosis in macrophages remains unclear and warrants further investigation.

Another possible implication of the DBP-induced increase in cell-surface CD36 is M2 skewing of the macrophage population. Macrophages treated with M2 stimuli exhibit increased expression of CD36 (Martinez *et al.* 2006, Vats *et al.* 2006, Oh *et al.* 2012,

Huang *et al.* 2014). In some models M2 activation of macrophages has been reported to be dependent on CD36 expression, with M2 stimulation of CD36-deficient macrophages resulting in reduced levels of M2 characteristics compared with CD36-competent cells (Oh *et al.* 2012, Huang *et al.* 2014). Inhibiting CD36 provided similar results, blocking the induction of M2 markers and traits following M2 stimulation (Huang *et al.* 2014).

5.2 The role of PPARγ in DBP-induced effects

CD36 is a known PPARγ target gene (Tontonoz *et al.* 1998), and thus a possible candidate for mediating the observed effects of DBP (Olderbø 2015). Indeed, in the present study, the known PPARγ agonists rosiglitazone and 15d-PGJ_2 markedly increased PMA-induced expression of cell-surface CD36 in a dose-dependent manner. In comparison, DBP only moderately increased CD36 expression at the highest dose, indicating that DBP only has weak agonistic potential. In accordance with these data, rosiglitazone substantially increased PPARγ co-activator recruitment in a cell-free system, while DBP only led to a slight increase at the highest doses (Kusu *et al.* 2008). Likewise, DBP was identified as a PPARγ activator in a reporter gene assay, exhibiting a relatively weak activating potential compared with rosiglitazone (Fang *et al.* 2015), further establishing DBP as a weak PPARγ agonist.

In the present study, exposure to rosiglitazone in combination with DBP reduced the effects of rosiglitazone on CD36 expression, indicating that DBP may act as an antagonist when applied in combination with a stronger agonist. Correspondingly, DBP exhibited antagonistic properties when used in combination with rosiglitazone in a cell-free PPARγ co-activator recruitment assay, diminishing the effects of rosiglitazone on co-activator recruitment (Kusu *et al.* 2008). Rosiglitazone is a full synthetic agonist that activates PPARγ through interactions with the canonical ligand-binding site (Nolte *et al.* 1998, Bruning *et al.* 2007, Hughes *et al.* 2014). Thus, the observed antagonistic effects of DBP suggest that DBP may interfere with rosiglitazone in its interaction with the PPARγ-LBD by displacing it in the canonical ligand-binding site (Figure 12A).

In contrast to rosiglitazone, combined exposure with 15d-PGJ_2 and DBP appeared to cause an additive effect where DBP augmented the effect of the endogenous ligand. 15d-PGJ_2 binds covalently to the Cys285 residue of helix 3 and activates the receptor through

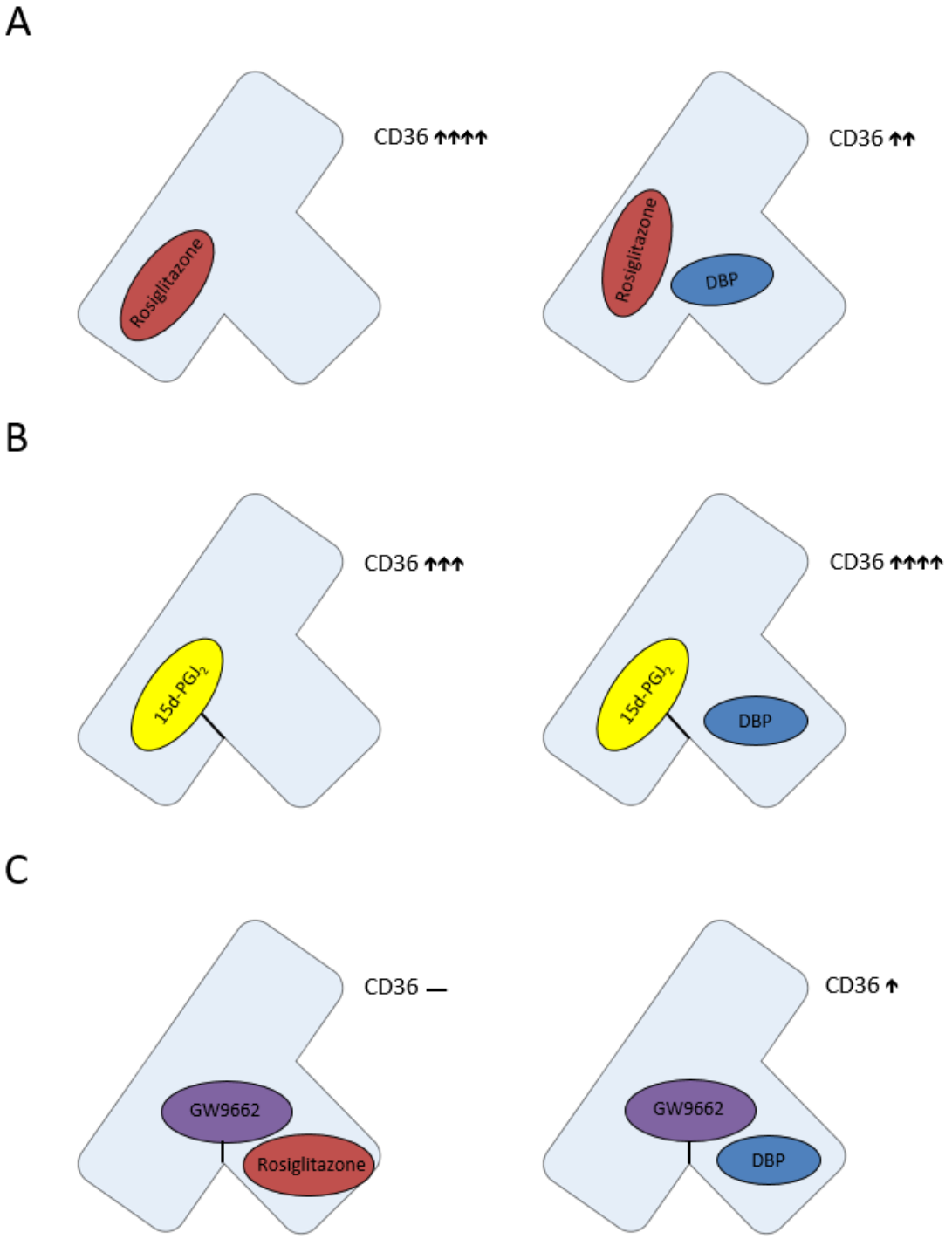

Figure 12. Schematic illustration of the postulated interactions of DBP with the PPARγ ligand-binding domain. The light blue area represents the PPARγ-LBD (See Figure 1 for a more detailed description). Arrows (↑) at the top right of each figure indicate the amount of cell-surface CD36 induced by each experimental treatment, while dash (–) represents no change in CD36. (A) DBP (blue) displaces rosiglitazone (red) from the canonical ligand-binding site and reduces the level of induced CD36. (B) DBP increases the basal induction of CD36 by 15d-PGJ_2 (yellow) through interactions with the alternative ligand-binding site. (C) The covalent antagonist GW9662 (purple) effectively blocks rosiglitazone, while DBP still induces low levels of CD36 through the alternative ligand-binding site.

interactions with the canonical ligand-binding site (Shiraki *et al.* 2005, Waku *et al.* 2009). This suggests that DBP may activate the receptor through interactions with the alternative ligand-binding site if the canonical ligand-binding site is unavailable (Figure 12B). Accordingly, the binding of multiple ligands in the same PPARγ-LBD is described in a number of studies (Itoh *et al.* 2008, Waku *et al.* 2010, Hughes *et al.* 2014). Certain partial agonists may bind to the alternative ligand-binding site if the canonical ligand-binding site is occupied by another ligand or blocked by a covalent agonist or antagonist (Itoh *et al.* 2008, Waku *et al.* 2010, Hughes *et al.* 2014). Moreover, the binding of a second ligand after covalent modification by an agonist has been reported to result in additional activation of the receptor (Waku *et al.* 2010, Hughes *et al.* 2014).

Further support for the interaction of DBP with the alternative ligand-binding site is provided by pre-incubation with the antagonist GW9662, which blocks the canonical ligand-binding site through covalent modification of the Cys285 residue of helix 3 (Leesnitzer *et al.* 2002). When applied in combination with DBP the antagonist failed to supress the effect on CD36, while the same doses effectively inhibited the effect of rosiglitazone (Figure 12C). In a similar manner, GW9662 blocked the transactivation potential of rosiglitazone in a luciferase reporter assay, while partial agonists with affinity for the alternative ligand-binding site were not inhibited (Hughes *et al.* 2014). Moreover, inhibition of rosiglitazone-induced co-activator recruitment by GW9662 was detected by Kusu *et al.* (2008) at a similar dose-range as used in the present study.

DBP, rosiglitazone and 15d-PGJ_2 did not affect the level of cell-surface CD36 in undifferentiated THP-1 monocytes. As the activation of the receptor is assumed to result in induction of CD36, a possible interpretation could be that these effects are independent of PPARγ. However, the transport of CD36 and the subsequent expression on the cell surface requires glycosylation of intracellular CD36, which increases during differentiation of monocytes to macrophages (Alessio *et al.* 1996). Consequently, PPARγ may be activated prior to PMA-differentiation in THP-1 monocytes, with any induced CD36 residing in a subcellular compartment as a less glycosylated precursor. Thus, this finding is not in conflict with the hypothesis of PPARγ activation.

In contrast to the effects on CD36, the amount of activated PPARγ in nuclear extracts from cells exposed to rosiglitazone or 15d-PGJ_2 were no greater than control, suggesting that the observed effects on CD36 are independent of PPARγ. However, this scenario

seems unlikely given the status of rosiglitazone and 15d-PGJ_2 as strong PPARγ agonists and potent inducers of CD36 (Chawla *et al.* 2001). Thus, a more likely explanation for the lack of activated PPARγ in the nuclear extracts is that the PPARγ activation assay, as used in the present study, was not optimal for detecting activated PPARγ in the applied model system. For instance, the DNA coating of the wells in the assay may contain a PPRE region of a promoter not recognized by the activated PPARγ complex induced in the current model (See appendix 4.4 for full discussion).

Even though the effects of rosiglitazone and 15d-PGJ_2 on CD36 are likely to be mediated through PPARγ, the results of the present study cannot fully exclude the possibility that DBP acts through other mechanisms or interacts with other signalling pathways that may account for the observed effects on CD36. In other model systems, CD36 has been reported to be regulated by the oestrogen receptor (ER) and aryl hydrocarbon receptor (AhR) signalling pathways (Uray *et al.* 2004, He *et al.* 2011), both of which can be activated by DBP (Takeuchi *et al.* 2005, Krüger *et al.* 2008, Ghisari and Bonefeld-Jorgensen 2009, Shen *et al.* 2009, Mankidy *et al.* 2013, Teixeira *et al.* 2015). Alternatively, DBP could affect the activation or inactivation of PPARγ indirectly by influencing its cofactors. DBP has been reported to induce the transcription of extracellular signal-regulated kinase 2 (ERK-2) in macrophages (Teixeira *et al.* 2015), which modulates the transcriptional activity of PPARγ through phosphorylation (Chen *et al.* 2003, Kim *et al.* 2013). Moreover, DBP induces oxidative stress (Seo *et al.* 2004, Xu *et al.* 2013), which has been reported to activate the PPARγ transcriptional co-activator nuclear factor erythroid 2–related factor 2 (NRF2) (Kim *et al.* 2013, Ma 2013). However, the fact that DBP affected CD36 in a manner consistent with the PPARγ-LBD literature and that similar effects have been reported for rosiglitazone in a PPARγ co-activator recruitment assay (Kusu *et al.* 2008) strongly suggests that the observed effects are due to PPARγ activation. Moreover, DBP induced several proteins regulated by PPARγ in a SILAC (Stable isotope labelling with amino acids in cell culture) assay performed previously in our lab (unpublished data), further supporting activation of PPARγ in the current model system.

In summary, there are several arguments supporting that the effect of DBP on cell-surface CD36 is mediated through interaction with PPARγ. (i) DBP induces CD36, a gene under regulatory control of PPARγ, albeit not as strongly as the known PPARγ agonists

rosiglitazone and 15d-PGJ_2, indicating weak agonistic properties. (ii) DBP attenuates the effects of rosiglitazone, possibly by displacing it in the canonical ligand-binding site. (iii) In addition, DBP augments the effects of 15d-PGJ_2, indicating that DBP may bind to the alternative ligand-binding site if the canonical ligand-binding site is blocked, further activating the receptor. (iv) Moreover, DBP enhances the expression of CD36 in the presence of the antagonist GW9662, also indicating affinity for the alternative ligand-binding site. Taken together, the current data suggest that DBP may act as a weak partial PPARγ agonist that can sample multiple binding configurations, and interact with both the canonical and the alternative ligand-binding site. In line with this conclusion, synthetic partial agonists have been reported to sample multiple binding configurations of similar affinity, correlating with their activating potential (Hughes *et al.* 2012), and to bind the alternative ligand-binding site with higher affinity than full synthetic agonists (Hughes *et al.* 2014).

The activation of PPARγ in airway macrophages may have implications of biological significance. Activation of M2 macrophages is associated with PPARγ signalling (Bouhlel *et al.* 2007, Odegaard *et al.* 2007), further supporting the notion that exposure to DBP may alter the macrophage activation state. In human monocyte-derived macrophages, activation of PPARγ during differentiation primed the cells for M2 activation (Bouhlel *et al.* 2007). However, activation of PPARγ did not affect the expression of M2 markers in resting or M1 macrophages (Bouhlel *et al.* 2007). In mouse macrophages, PPARγ was required for maturation of M2 macrophages, with PPARγ-deficient mice displaying reduced levels of M2 markers and traits following M2 stimulation (Odegaard *et al.* 2007). In addition, rosiglitazone enhanced induction of the M2 marker arginase-1 by M2 stimuli in mouse macrophages transfected with a luciferase reporter (Odegaard *et al.* 2007).

5.3 Implications of DBP-induced M2 skewing in the airways

As previously stated, both the enhanced levels of CD36 induced by DBP and the presumed activation of PPARγ may imply increased M2 skewing of the macrophage population. M2 macrophages are implicated in the pathogenesis of asthma and are likely to play a role in the tissue remodelling associated with the disease, although their exact

role is currently unknown (Byers and Holtzman 2010, Sica and Mantovani 2012). Biopsy specimens from the lungs of asthmatic patients with reduced lung function contained more M2 macrophages than the lungs of healthy subjects (Melgert *et al.* 2011). Moreover, an increase in M2-associated gene expression was observed in children undergoing severe asthma exacerbation (Subrata *et al.* 2009). In mice, the adoptive transfer of M2 macrophages enhances TH_2-mediated inflammation in models of allergic airway inflammation (Melgert *et al.* 2010, Ford *et al.* 2012). Moreover, inhibiting M2 differentiation prior to adoptive transfer of macrophages is associated with increased protection from allergic airway disease in *aspergillus fumigatus* sensitized mice (Moreira *et al.* 2010). Thus, it is tempting to speculate that the priming of macrophages for M2 differentiation through activation of PPARγ provides a possible link between exposure to DBP and its respiratory effects.

5.4 Limitations and future studies

Although CD36 is under the transcriptional control of PPARγ (Tontonoz *et al.* 1998, Chawla *et al.* 2001), increased expression of CD36 is only indicative of PPARγ activation. Similarly, while the combined exposure with PPARγ agonists and antagonists suggest a role for PPARγ in the observed effects on CD36, it does not reveal the specific interactions with the PPARγ-LBD. Further work is needed to establish PPARγ activation by DBP in the current model, replacing the PPARγ activation assay unsuccessfully applied in the present study (For full description, see Appendix 4). An alternative method for demonstrating PPARγ activation in the current model system would be transfection with a luciferase reporter (Feige *et al.* 2007). It would be particularly interesting to show activation of PPARγ by DBP in the presence of GW9662, thus confirming interactions with the alternative ligand-binding site. Other model systems have succeeded in demonstrating that DBP acts as a PPARγ agonist and may provide an alternative to the assay applied currently (Kusu *et al.* 2008, Fang *et al.* 2015). For instance, successfully replicating the effects described in the current study in an assay directly assessing PPARγ activation would strengthen the conclusions drawn based on the induction of CD36 alone. To fully explore the interaction with PPARγ, further studies using crystallography supplemented with nuclear magnetic resonance and hydrogen deuterium exchange could be applied to reveal the mode of binding in the PPARγ-LBD

and which structures are stabilized, following binding of DBP alone or in combination with either rosiglitazone, 15d-PGJ_2 or GW9662 (Bruning *et al.* 2007, Hughes *et al.* 2012, Hughes *et al.* 2014).

The results and conclusions presented in the present study rely heavily on the use of the THP-1 cell line. THP-1 monocytes can be differentiated into macrophage-like cells using PMA, and offer advantages over primary macrophages such as low cost, ease of *ex vivo* propagation and reproducibility. However, a number of differences have been reported between THP-1 cells and human monocyte-derived macrophages, including differential gene expression, morphology and functions (Kohro *et al.* 2004, Daigneault *et al.* 2010). As a consequence, the main results obtained in the present study should be verified in human primary monocyte-derived macrophages to confirm the biological relevance of the results (Teixeira *et al.* 2015).

Rough estimates of pulmonary DBP exposure have been reported to be in the range of approximately 0.03 μM to 4 μM (Bølling *et al.* 2013). Consequently, the concentrations of DBP applied in the present study are likely to be higher than those expected in the human lung due to indoor inhalation exposure. However, DBP concentrations between 0.01 μM to 10 μM have been reported to affect primary and monocyte-derived macrophages (Li *et al.* 2013, Teixeira *et al.* 2015, Steensen 2016), suggesting that the THP-1 cells applied here may be more robust than primary macrophage models. This further emphasizes the need to confirm the current results in human monocyte-derived macrophages.

In the present study the expression of cell-surface CD36 was used to infer effects on macrophage function and activation. However, additional experiments using more specialized markers are required to fully characterize the effect of DBP on these endpoints. Repeating the flow cytometry analysis applied in the present study using a specific M2 marker, such as CD206 (C-type mannose receptor 1), may ascertain the ability of DBP to influence the macrophage activation state (Murray *et al.* 2014). As a prototypic M2 stimulus, IL-4 could potentially be used as a positive control for M2 activation (Murray *et al.* 2014). To assess the effect of DBP on the phagocytic capacity of macrophages, a phagocytosis assay using apoptotic cells or particles with motifs recognized by CD36 could be applied (Fadok *et al.* 1998, Li *et al.* 2013, Couleau *et al.* 2015, Woo *et al.* 2016). In macrophages CD36 is a high affinity receptor that mediates

uptake, binding and degradation of oxLDL (Endemann *et al.* 1993), suggesting that exposure to DBP may possibly increase the uptake of oxLDL through enhanced expression of CD36. Uptake of oxLDL in macrophages through CD36 is implicated in the formation of foam cells, which are associated with the pathogenesis of atherosclerosis (Park 2014). Accordingly, it would be interesting to investigate the ability of DBP to influence the uptake of oxLDL.

If the results are ascertained in primary cells, it would be interesting to assess the ability of DBP to induce or exacerbate asthma and related symptoms in a mouse model of allergic airway inflammation. For instance, inhalation exposure to DBP prior to allergic sensitization may be applied to assess possible adjuvant effects on airway symptoms (Kurahashi *et al.* 2005, Guo *et al.* 2012, Han *et al.* 2014). Additionally, severe combined immunodeficiency (SCID) mice lacking lymphocytes could be used to determine the contribution of the effect on macrophages alone (Mills *et al.* 2000).

6 Conclusions

The results reported in the present study strongly suggest that the observed increase in CD36 induced by DBP is mediated by PPARγ. DBP slightly enhanced the expression of CD36, indicating weak agonistic potential. When administered together with rosiglitazone, DBP attenuated the effect of the reversibly binding agonist. In contrast, during combined exposure with the covalently binding agonist 15d-PGJ_2, DBP appeared to cause an additive increase in cell-surface CD36. Finally, DBP also increased the expression of CD36 in the presence of the covalently bound antagonist GW9662. The reduction in the effects of rosiglitazone on CD36 indicates that DBP may displace a reversibly bound agonist in the canonical ligand-binding site, while the DBP-induced increase in CD36 in the presence of the covalently bound ligands 15d-PGJ_2 and GW9662 indicates affinity for the alternative ligand-binding site. In conclusion, the current data suggests that DBP acts as a weak partial PPARγ agonist that may sample multiple binding-configurations and activate the receptor through interactions with both the canonical and alternative ligand-binding site. Nevertheless, further verification in other model systems is required to fully elucidate the interaction of DBP with PPARγ and its role in the macrophage differentiation process.

Both the observed increase in cell-surface CD36 and the alleged activation of PPARγ may indicate increased M2 skewing of the macrophage population. Although their role in the disease is not fully understood at the present, M2 macrophages are associated with the pathogenesis of asthma and may form a link between exposure to DBP and the observed association with airway effects. In addition to its role in airway immunology, PPARγ is associated with conditions such as atherosclerosis, diabetes, obesity and metabolic disorders. Thus, possible associations between exposure to DBP and these diseases warrant further investigation.

References

Aci-Sèche, S., M. Genest and N. Garnier (2011). "Ligand entry pathways in the ligand binding domain of PPARγ receptor." *Federation of European Biochemical Societies Letters* **585**(16): 2599-2603.

Alessio, M., L. De Monte, A. Scirea, P. Gruarin, N. N. Tandon and R. Sitia (1996). "Synthesis, processing, and intracellular transport of CD36 during monocytic differentiation." *Journal of Biological Chemistry* **271**(3): 1770-1775.

Anderson, W., L. Castle, M. Scotter, R. Massey and C. Springall (2001). "A biomarker approach to measuring human dietary exposure to certain phthalate diesters." *Food Additives & Contaminants* **18**(12): 1068-1074.

Asada, K., S. Sasaki, T. Suda, K. Chida and H. Nakamura (2004). "Antiinflammatory roles of peroxisome proliferator–activated receptor γ in human alveolar macrophages." *American Journal of Respiratory and Critical Care Medicine* **169**(2): 195-200.

Asher, M. I., S. Montefort, B. Björkstén, C. K. Lai, D. P. Strachan, S. K. Weiland, H. Williams and I. P. T. S. Group (2006). "Worldwide time trends in the prevalence of symptoms of asthma, allergic rhinoconjunctivitis, and eczema in childhood: ISAAC Phases One and Three repeat multicountry cross-sectional surveys." *The Lancet* **368**(9537): 733-743.

Auwerx, J. (1991). "The human leukemia cell line, THP-1: a multifacetted model for the study of monocyte-macrophage differentiation." *Experientia* **47**(1): 22-31.

Becker, J., C. Delayre-Orthez, N. Frossard and F. Pons (2006). "Regulation of inflammation by PPARs: a future approach to treat lung inflammatory diseases?" *Fundamental & Clinical Pharmacology* **20**(5): 429-447.

Bekö, G., M. Callesen, C. J. Weschler, J. Toftum, S. Langer, T. Sigsgaard, A. Høst, T. K. Jensen and G. Clausen (2015). "Phthalate exposure through different pathways and allergic sensitization in preschool children with asthma, allergic rhinoconjunctivitis and atopic dermatitis." *Environmental Research* **137**: 432-439.

Bertelsen, R. J., K. C. L. Carlsen, A. M. Calafat, J. A. Hoppin, G. Håland, P. Mowinckel, K.-H. Carlsen and M. Løvik (2013). "Urinary biomarkers for phthalates associated with asthma in Norwegian children." *Environmental Health Perspectives* **121**(2): 251-256.

Bornehag, C.-G., J. Sundell, L. Hagerhed-Engman, T. Sigsggard, S. Janson and N. Aberg (2005). "'Dampness' at home and its association with airway, nose, and skin symptoms among 10,851 preschool children in Sweden: a cross-sectional study." *Indoor Air* **15**(s10): 48-55.

Bornehag, C.-G., J. Sundell, C. J. Weschler, T. Sigsgaard, B. Lundgren, M. Hasselgren and L. Hägerhed-Engman (2004). "The association between asthma and allergic symptoms in children and phthalates in house dust: a nested case-control study." *Environmental Health Perspectives* **112**(14): 1393-1397.

Bouhlel, M. A., B. Derudas, E. Rigamonti, R. Dièvart, J. Brozek, S. Haulon, C. Zawadzki, B. Jude, G. Torpier and N. Marx (2007). "PPARγ activation primes human monocytes into alternative M2 macrophages with anti-inflammatory properties." *Cell Metabolism* **6**(2): 137-143.

Bruning, J. B., M. J. Chalmers, S. Prasad, S. A. Busby, T. M. Kamenecka, Y. He, K. W. Nettles and P. R. Griffin (2007). "Partial agonists activate PPARγ using a helix 12 independent mechanism." *Structure* **15**(10): 1258-1271.

Bruyère, C., S. Madonna, G. Van Goietsenoven, V. Mathieu, J. Dessolin, J.-L. Kraus, F. Lefranc and R. Kiss (2011). "JLK1486, a bis 8-hydroxyquinoline-substituted benzylamine, displays cytostatic effects in experimental gliomas through MyT1 and STAT1 activation and, to a lesser extent, PPARγ activation." *Translational Oncology* **4**(3): 126–137.

Burnette, W. N. (1981). ""Western blotting": electrophoretic transfer of proteins from sodium dodecyl sulfate-polyacrylamide gels to unmodified nitrocellulose and radiographic detection with antibody and radioiodinated protein A." *Analytical Biochemistry* **112**(2): 195-203.

Byers, D. E. and M. J. Holtzman (2010). "Alternatively activated macrophages as cause or effect in airway disease." *American Journal of Respiratory Cell and Molecular Biology* **43**(1): 1-4.

Bølling, A. K., J. A. Holme, C. G. Bornehag, U. C. Nygaard, R. J. Bertelsen, E. Nånberg, J. Bodin, A. K. Sakhi, C. Thomsen and R. Becher (2013). "Pulmonary phthalate exposure and asthma-is PPAR a plausible mechanistic link?" *Experimental and Clinical Sciences* **12**: 733-759.

Chalubinski, M. and M. Kowalski (2006). "Endocrine disrupters–potential modulators of the immune system and allergic response." *Allergy* **61**(11): 1326-1335.

Chawla, A., Y. Barak, L. Nagy, D. Liao, P. Tontonoz and R. M. Evans (2001). "PPAR-γ dependent and independent effects on macrophage-gene expression in lipid metabolism and inflammation." *Nature Medicine* **7**(1): 48-52.

Chen, F., M. Wang, J. P. O'Connor, M. He, T. Tripathi and L. E. Harrison (2003). "Phosphorylation of PPARγ via active ERK1/2 leads to its physical association with p65 and inhibition of NF-κβ." *Journal of Cellular Biochemistry* **90**(4): 732-744.

Couleau, N., J. Falla, A. Beillerot, E. Battaglia, M. D'innocenzo, S. Plançon, P. Laval-Gilly and A. Bennasroune (2015). "Effects of endocrine disruptor compounds, alone or in combination, on human macrophage-like THP-1 cell response." *PloS one* **10**(7): e0131428. doi:0131410.0131371/journal.pone.0131428.

Cox, J. C. and A. R. Coulter (1997). "Adjuvants—a classification and review of their modes of action." *Vaccine* **15**(3): 248-256.

CPSC (2008). "Consumer product safety improvement act of 2008 " US consumer product safety commission (CPSC). Retrieved 25/5, 2017, from https://www.cpsc.gov/en/Regulations-Laws--Standards/Statutes/The-Consumer-Product-Safety-Improvement-Act/.

Croisant, S. (2014). Epidemiology of asthma: prevalence and burden of disease. *Heterogeneity in Asthma*. A. R. Brasier, Springer**:** 17-29.

Daigneault, M., J. A. Preston, H. M. Marriott, M. K. Whyte and D. H. Dockrell (2010). "The identification of markers of macrophage differentiation in PMA-stimulated THP-1 cells and monocyte-derived macrophages." *PloS one* **5**(1): e8668. doi:8610.1371/journal.pone.0008668.

ECHA (2010). "Evaluation of new scientific evidence concerning the restrictions contained in anex XVII to regulation (EC) NO 1907/2006 (REACH)." European Chemicals Agency (ECHA). Retrieved 25/5, 2017, from https://echa.europa.eu/documents/10162/13641/dbp_echa_review_report_2010_6_en.pdf.

Endemann, G., L. Stanton, K. Madden, C. Bryant, R. T. White and A. Protter (1993). "CD36 is a receptor for oxidized low density lipoprotein." *Journal of Biological Chemistry* **268**(16): 11811-11816.

ERS (2013). "THE EUROPEAN LUNG white book". G. John Gibson, R. Loddenkemper, Y. Sibille, B. Lundback, European Respiratory Society (ERS).

EU (2005). "Directive 2005/84/EC of the European Parliament and of the Council of 14 December 2005 amending for the 22nd time Council Directive 76/769/EEC on the approximation of the laws, regulations and administrative provisions of the Member States relating to restrictions on the marketing and use of certain dangerous substances and preparations (phthalates in toys and childcare articles)." European Parliament and the Council of the European Union (EU). Retrieved 25/5, 2017, from http://eur-lex.europa.eu/legal-content/EN/ALL/?uri=celex:32005L0084.

EU (2009). "Regulation (EC) No 1223/2009 of the European Parliament and of the Council of 30 November 2009 on cosmetic products." European Parliament and the Council of the European Union (EU).

Retrieved 25/5, 2017, from http://eur-lex.europa.eu/legal-content/EN/TXT/?uri=CELEX:32009R1223&qid=1468315857067.

Fadok, V. A., M. L. Warner, D. L. Bratton and P. M. Henson (1998). "CD36 is required for phagocytosis of apoptotic cells by human macrophages that use either a phosphatidylserine receptor or the vitronectin receptor (αvβ3)." *The Journal of Immunology* **161**(11): 6250-6257.

Fajas, L., D. Auboeuf, E. Raspé, K. Schoonjans, A.-M. Lefebvre, R. Saladin, J. Najib, M. Laville, J.-C. Fruchart and S. Deeb (1997). "The organization, promoter analysis, and expression of the human PPARγ gene." *Journal of Biological Chemistry* **272**(30): 18779-18789.

Fang, M., T. F. Webster and H. M. Stapleton (2015). "Activation of human peroxisome proliferator-activated nuclear receptors (PPARγ1) by semi-volatile compounds (SVOCs) and chemical mixtures in indoor dust." *Environmental Science & Technology* **49**(16): 10057-10064.

Febbraio, M., D. P. Hajjar and R. L. Silverstein (2001). "CD36: a class B scavenger receptor involved in angiogenesis, atherosclerosis, inflammation, and lipid metabolism." *The Journal of Clinical Investigation* **108**(6): 785-791.

Feige, J., L. Gelman, L. Michalik, B. Desvergne and W. Wahli (2006). "From molecular action to physiological outputs: PPAR are nuclear receptors at the crossroads of key cellular functions." *Progress in Lipid Research* **45**(2): 120-159.

Feige, J. N., L. Gelman, D. Rossi, V. Zoete, R. Métivier, C. Tudor, S. I. Anghel, A. Grosdidier, C. Lathion and Y. Engelborghs (2007). "The endocrine disruptor monoethyl-hexyl-phthalate is a selective peroxisome proliferator-activated receptor γ modulator that promotes adipogenesis." *Journal of Biological Chemistry* **282**(26): 19152-19166.

Ford, A. Q., P. Dasgupta, I. Mikhailenko, E. M. Smith, N. Noben-Trauth and A. D. Keegan (2012). "Adoptive transfer of IL-4Rα+ macrophages is sufficient to enhance eosinophilic inflammation in a mouse model of allergic lung inflammation." *BMC Immunology* **13**(1): 6. doi:10.1186/1471-2172-1113-1186.

Franken, C., N. Lambrechts, E. Govarts, G. Koppen, E. Den Hond, D. Ooms, S. Voorspoels, L. Bruckers, I. Loots and V. Nelen (2017). "Phthalate-induced oxidative stress and association with asthma-related airway inflammation in adolescents." *International Journal of Hygiene and Environmental Health* **220**(2): 468–477.

Frederiksen, H., T. K. Jensen, N. Jørgensen, H. B. Kyhl, S. Husby, N. E. Skakkebæk, K. M. Main, A. Juul and A.-M. Andersson (2014). "Human urinary excretion of non-persistent environmental chemicals: an overview of Danish data collected between 2006 and 2012." *Reproduction* **147**(4): 555-565.

Frederiksen, H., N. E. Skakkebaek and A. M. Andersson (2007). "Metabolism of phthalates in humans." *Molecular Nutrition & Food Research* **51**(7): 899-911.

Fromme, H. (2011). Phthalates: Human Exposure. *Encyclopedia of Environmental Health*. J. O. Nriagu, Newnes**:** 498-510.

Fromme, H., T. Lahrz, M. Piloty, H. Gebhart, A. Oddoy and H. Rüden (2004). "Occurrence of phthalates and musk fragrances in indoor air and dust from apartments and kindergartens in Berlin (Germany)." *Indoor Air* **14**(3): 188-195.

Genest, D., N. Garnier, A. Arrault, C. Marot, L. Morin-Allory and M. Genest (2008). "Ligand-escape pathways from the ligand-binding domain of PPARγ receptor as probed by molecular dynamics simulations." *European Biophysics Journal* **37**(4): 369-379.

Genuis, S. J., S. Beesoon, R. A. Lobo and D. Birkholz (2012). "Human elimination of phthalate compounds: blood, urine, and sweat (BUS) study." *The Scientific World Journal* **2012**: 615068. doi:615010.611100/612012/615068.

Ghisari, M. and E. C. Bonefeld-Jorgensen (2009). "Effects of plasticizers and their mixtures on estrogen receptor and thyroid hormone functions." *Toxicology Letters* **189**(1): 67-77.

Giam, C., E. Atlas, M. Powers Jr and J. E. Leonard (1984). Phthalic acid esters. *Anthropogenic Compounds*, Springer**:** 67-142.

Guo, J., B. Han, L. Qin, B. Li, H. You, J. Yang, D. Liu, C. Wei, E. Nanberg and C.-G. Bornehag (2012). "Pulmonary toxicity and adjuvant effect of di-(2-exylhexyl) phthalate in ovalbumin-immunized BALB/c mice." *PloS one* **7**(6): e39008. doi: 39010.31371/journal.pone.0039008.

Han, Y., X. Wang, G. Chen, G. Xu, X. Liu, W. Zhu, P. Hu, Y. Zhang, C. Zhu and J. Miao (2014). "Di-(2-ethylhexyl) phthalate adjuvantly induces imbalanced humoral immunity in ovalbumin-sensitized BALB/c mice ascribing to T follicular helper cells hyperfunction." *Toxicology* **324**: 88-97.

Hasegawa, H., Y. Yamada, K. Komiyama, M. Hayashi, M. Ishibashi, T. Sunazuka, T. Izuhara, K. Sugahara, K. Tsuruda and M. Masuda (2007). "A novel natural compound, a cycloanthranilylproline derivative (Fuligocandin B), sensitizes leukemia cells to apoptosis induced by tumor necrosis factor–related apoptosis-inducing ligand (TRAIL) through 15-deoxy-Δ12, 14 prostaglandin J2 production." *Blood* **110**(5): 1664-1674.

Hauser, R., S. Duty, L. Godfrey-Bailey and A. M. Calafat (2004). "Medications as a source of human exposure to phthalates." *Environmental Health Perspectives* **112**(6): 751-753.

He, J., J. H. Lee, M. Febbraio and W. Xie (2011). "The emerging roles of fatty acid translocase/CD36 and the aryl hydrocarbon receptor in fatty liver disease." *Experimental Biology and Medicine* **236**(10): 1116-1121.

Hernandez-Diaz, S., A. A. Mitchell, K. E. Kelley, A. M. Calafat and R. Hauser (2009). "Medications as a Potential Source of Exposure to Phthalates in the US Population." *Environmental Health Perspectives* **117**(2): 185-189.

Hoppin, J. A., R. Ulmer and S. J. London (2004). "Phthalate exposure and pulmonary function." *Environmental Health Perspectives* **112**(5): 571–574.

Hsu, N. Y., C. C. Lee, J. Y. Wang, Y. C. Li, H. W. Chang, C. Y. Chen, C. G. Bornehag, P. C. Wu, J. Sundell and H. J. Su (2012). "Predicted risk of childhood allergy, asthma, and reported symptoms using measured phthalate exposure in dust and urine." *Indoor Air* **22**(3): 186-199.

Huang, S. C.-C., B. Everts, Y. Ivanova, D. O'sullivan, M. Nascimento, A. M. Smith, W. Beatty, L. Love-Gregory, W. Y. Lam and C. M. O'neill (2014). "Cell-intrinsic lysosomal lipolysis is essential for alternative activation of macrophages." *Nature Immunology* **15**: 846–855.

Hughes, T. S., M. J. Chalmers, S. Novick, D. S. Kuruvilla, M. R. Chang, T. M. Kamenecka, M. Rance, B. A. Johnson, T. P. Burris and P. R. Griffin (2012). "Ligand and receptor dynamics contribute to the mechanism of graded PPARγ agonism." *Structure* **20**(1): 139-150.

Hughes, T. S., P. K. Giri, I. M. S. De Vera, D. P. Marciano, D. S. Kuruvilla, Y. Shin, A.-L. Blayo, T. M. Kamenecka, T. P. Burris and P. R. Griffin (2014). "An alternate binding site for PPARγ ligands." *Nature Communications* **5**: 3571. doi:3510.1038/ncomms4571.

Hume, D. A. (2015). "The many alternative faces of macrophage activation." *Frontiers in Immunology* **6**: 370. doi:310.3389/fimmu.2015.00370.

Hurst, C. H. and D. J. Waxman (2003). "Activation of PPARα and PPARγ by environmental phthalate monoesters." *Toxicological Sciences* **74**(2): 297-308.

Högberg, J., A. Hanberg, M. Berglund, S. Skerfving, M. Remberger, A. M. Calafat, A. F. Filipsson, B. Jansson, N. Johansson and M. Appelgren (2008). "Phthalate diesters and their metabolites in human breast milk, blood or serum, and urine as biomarkers of exposure in vulnerable populations." *Environmental Health Perspectives* **116**(3): 334–339.

Itoh, T., L. Fairall, K. Amin, Y. Inaba, A. Szanto, B. L. Balint, L. Nagy, K. Yamamoto and J. W. Schwabe (2008). "Structural basis for the activation of PPARγ by oxidized fatty acids." *Nature Structural & Molecular Biology* **15**(9): 924-931.

Jurewicz, J. and W. Hanke (2011). "Exposure to phthalates: Reproductive outcome and children health. A review of epidemiological studies." *International Journal of Occupational Medicine and Environmental Health* **24**(2): 115-141.

Jaakkola, J., P. K. Verkasalo and N. Jaakkola (2000). "Plastic wall materials in the home and respiratory health in young children." *American Journal of Public Health* **90**(5): 797–799.

Jaakkola, J. J. and T. L. Knight (2008). "The role of exposure to phthalates from polyvinyl chloride products in the development of asthma and allergies: a systematic review and meta-analysis." *Environmental Health Perspectives* **116**(7): 845–853.

Jaakkola, J. J., H. Parise, V. Kislitsin, N. I. Lebedeva and J. D. Spengler (2004). "Asthma, wheezing, and allergies in Russian schoolchildren in relation to new surface materials in the home." *American Journal of Public Health* **94**(4): 560-562.

Kim, H. G., S.-m. Yeon, K. H. Kim, H. Kim, J.-I. Park, H.-J. Kang, E. J. Cha, H.-D. Park, H. J. Kang and T. W. Park (2015). "Estrogenic endocrine-disrupting chemicals modulate the production of inflammatory mediators and cell viability of lipopolysaccharide-stimulated macrophages." *Inflammation* **38**(2): 595-605.

Kim, T.-H., M.-Y. Kim, S.-H. Jo, J.-M. Park and Y.-H. Ahn (2013). "Modulation of the Transcriptional Activity of Peroxisome Proliferator-Activated Receptor Gamma by Protein-Protein Interactions and Post-Translational Modifications." *Yonsei Medical Journal* **54**(3): 545-559.

Kimber, I. and R. J. Dearman (2010). "An assessment of the ability of phthalates to influence immune and allergic responses." *Toxicology* **271**(3): 73-82.

Koch, H. M., K. L. Y. Christensen, V. Harth, M. Lorber and T. Brüning (2012). "Di-n-butyl phthalate (DnBP) and diisobutyl phthalate (DiBP) metabolism in a human volunteer after single oral doses." *Archives of Toxicology* **86**(12): 1829-1839.

Kohro, T., T. Tanaka, T. Murakami, Y. Wada, H. Aburatani, T. Hamakubo and T. Kodama (2004). "A comparison of differences in the gene expression profiles of phorbol 12-myristate 13-acetate differentiated THP-1 cells and human monocyte-derived macrophage." *Journal of Atherosclerosis and Thrombosis* **11**(2): 88-97.

Krey, G., O. Braissant, F. L'Horset, E. Kalkhoven, M. Perroud, M. G. Parker and W. Wahli (1997). "Fatty acids, eicosanoids, and hypolipidemic agents identified as ligands of peroxisome proliferator-activated receptors by coactivator-dependent receptor ligand assay." *Molecular Endocrinology* **11**(6): 779-791.

Krüger, T., M. Long and E. C. Bonefeld-Jørgensen (2008). "Plastic components affect the activation of the aryl hydrocarbon and the androgen receptor." *Toxicology* **246**(2): 112-123.

Kurahashi, N., T. Kondo, M. Omura, T. Umemura, M. Ma and R. Kishi (2005). "The effects of subacute inhalation of di (2-ethylhexyl) phthalate (DEHP) on the testes of prepubertal Wistar rats." *Journal of Occupational Health* **47**(5): 437-444.

Kusu, R., A. Oishi, K. Kakizawa, T. Kimura, C. Toda, K. Hashizume, K. Ueda and N. Kojima (2008). "Effects of phthalate ester derivatives including oxidized metabolites on coactivator recruiting by PPARα and PPARγ." *Toxicology in Vitro* **22**(6): 1534-1538.

Lampen, A., S. Zimnik and H. Nau (2003). "Teratogenic phthalate esters and metabolites activate the nuclear receptors PPARs and induce differentiation of F9 cells." *Toxicology and Applied Pharmacology* **188**(1): 14-23.

Leesnitzer, L. M., D. J. Parks, R. K. Bledsoe, J. E. Cobb, J. L. Collins, T. G. Consler, R. G. Davis, E. A. Hull-Ryde, J. M. Lenhard and L. Patel (2002). "Functional consequences of cysteine modification in the ligand binding sites of peroxisome proliferator activated receptors by GW9662." *Biochemistry* **41**(21): 6640-6650.

Lehner, K., F. Santarelli, R. Vasold, B. König, M. Landthaler and W. Bäumler (2011). "Black tattoo inks are a source of problematic substances such as dibutyl phthalate." *Contact Dermatitis* **65**(4): 231-238.

Li, L., H.-S. Li, N.-N. Song and H.-M. Chen (2013). "The immunotoxicity of dibutyl phthalate on the macrophages in mice." *Immunopharmacology and Immunotoxicology* **35**(2): 272-281.

Loftus, P. A. and S. K. Wise (2015). "Epidemiology and economic burden of asthma." *International Forum of Allergy & Rhinology* **5**(1): 7-10.

Ma, Q. (2013). "Role of nrf2 in oxidative stress and toxicity." *Annual Review of Pharmacology and Toxicology* **53**: 401-426.

Mankidy, R., S. Wiseman, H. Ma and J. P. Giesy (2013). "Biological impact of phthalates." *Toxicology Letters* **217**(1): 50-58.

Martin, T. R. and C. W. Frevert (2005). "Innate immunity in the lungs." *Proceedings of the American Thoracic Society* **2**(5): 403-411.

Martinez, F. O., S. Gordon, M. Locati and A. Mantovani (2006). "Transcriptional profiling of the human monocyte-to-macrophage differentiation and polarization: new molecules and patterns of gene expression." *The Journal of Immunology* **177**(10): 7303-7311.

Melgert, B. N., T. B. Oriss, Z. Qi, B. Dixon-McCarthy, M. Geerlings, M. N. Hylkema and A. Ray (2010). "Macrophages: regulators of sex differences in asthma?" *American Journal of Respiratory Cell and Molecular Biology* **42**(5): 595-603.

Melgert, B. N., N. H. ten Hacken, B. Rutgers, W. Timens, D. S. Postma and M. N. Hylkema (2011). "More alternative activation of macrophages in lungs of asthmatic patients." *Journal of Allergy and Clinical Immunology* **127**(3): 831-833.

Mills, C. D., K. Kincaid, J. M. Alt, M. J. Heilman and A. M. Hill (2000). "M-1/M-2 macrophages and the Th1/Th2 paradigm." *The Journal of Immunology* **164**(12): 6166-6173.

Moreira, A. P., K. A. Cavassani, R. Hullinger, R. S. Rosada, D. J. Fong, L. Murray, D. P. Hesson and C. M. Hogaboam (2010). "Serum amyloid P attenuates M2 macrophage activation and protects against fungal spore–induced allergic airway disease." *Journal of Allergy and Clinical Immunology* **126**(4): 712-721.

Murray, P. J., J. E. Allen, S. K. Biswas, E. A. Fisher, D. W. Gilroy, S. Goerdt, S. Gordon, J. A. Hamilton, L. B. Ivashkiv and T. Lawrence (2014). "Macrophage activation and polarization: nomenclature and experimental guidelines." *Immunity* **41**(1): 14-20.

Murray, P. J. and T. A. Wynn (2011). "Protective and pathogenic functions of macrophage subsets." *Nature Reviews Immunology* **11**(11): 723-737.

Nolte, R. T., G. B. Wisely, S. Westin, J. E. Cobb, M. H. Lambert, R. Kurokawa, M. G. Rosenfeld, T. M. Willson, C. K. Glass and M. V. Milburn (1998). "Ligand binding and co-activator assembly of the peroxisome proliferator-activated receptor-γ." *Nature* **395**(6698): 137-143.

Nuclear Receptors Nomenclature Committee (1999). "A unified nomenclature system for the nuclear receptor superfamily." *Cell* **97**(2): 161-163.

Odegaard, J. I., R. R. Ricardo-Gonzalez, M. H. Goforth, C. R. Morel, V. Subramanian, L. Mukundan, A. R. Eagle, D. Vats, F. Brombacher and A. W. Ferrante (2007). "Macrophage-specific PPARγ controls alternative activation and improves insulin resistance." *Nature* **447**(7148): 1116-1120.

Oh, J., A. E. Riek, S. Weng, M. Petty, D. Kim, M. Colonna, M. Cella and C. Bernal-Mizrachi (2012). "Endoplasmic reticulum stress controls M2 macrophage differentiation and foam cell formation." *Journal of Biological Chemistry* **287**(15): 11629-11641.

Olderbø, B. P. (2015). "Effects of di-n-butyl phthalate (DBP) on THP-1-derived macrophages." Master thesis, University of Oslo.

Orihara, K., N. Dil, V. Anaparti and R. Moqbel (2010). "What's new in asthma pathophysiology and immunopathology?" *Expert Review of Respiratory Medicine* **4**(5): 605-629.

Ormerod, M. G. (2008). "Flow cytometry - A Basic Introduction." Retrieved 25/5, 2017, from http://flowbook.denovosoftware.com/.

Otake, T., J. Yoshinaga and Y. Yanagisawa (2004). "Exposure to phthalate esters from indoor environment." *Journal of Exposure Science and Environmental Epidemiology* **14**(7): 524-528.

Pan, C., C. Kumar, S. Bohl, U. Klingmueller and M. Mann (2009). "Comparative proteomic phenotyping of cell lines and primary cells to assess preservation of cell type-specific functions." *Molecular & Cellular Proteomics* **8**(3): 443-450.

Parham, P. (2014). "The Immune System", 4th edition. New York, USA, Garland Science.

Park, Y. M. (2014). "CD36, a scavenger receptor implicated in atherosclerosis." *Experimental & Molecular Medicine* **46**(6): e99. doi:10.1038/emm.2014.1038.

Roche (2016). "Cytotoxicity Detection Kit (LDH)." Retrieved 21/8, 2016, from https://lifescience.roche.com/webapp/wcs/stores/servlet/ProductDisplay?partNumber=3.5.3.27.1.14.

Rőszer, T. (2015). "Understanding the mysterious M2 macrophage through activation markers and effector mechanisms." *Mediators of Inflammation* **2015**: 816460. doi:816410.811155/812015/816460.

Samokhvalov, V., J. Vriend, K. L. Jamieson, M. Akhnokh, R. Manne, J. R. Falck and J. M. Seubert (2014). "PPARγ signaling is required for mediating EETs protective effects in neonatal cardiomyocytes exposed to LPS." *Frontiers in Pharmacology* **5**: 242. doi:210.3389/fphar.2014.00242.

Schijns, V. E. (2003). "Mechanisms of vaccine adjuvant activity: initiation and regulation of immune responses by vaccine adjuvants." *Vaccine* **21**(9-10): 829–831.

Seckin, E., H. Fromme and W. Völkel (2009). "Determination of total and free mono-n-butyl phthalate in human urine samples after medication of a di-n-butyl phthalate containing capsule." *Toxicology Letters* **188**(1): 33-37.

Seo, K. W., K. B. Kim, Y. J. Kim, J. Y. Choi, K. T. Lee and K. S. Choi (2004). "Comparison of oxidative stress and changes of xenobiotic metabolizing enzymes induced by phthalates in rats." *Food and Chemical Toxicology* **42**(1): 107-114.

Shen, O., G. Du, H. Sun, W. Wu, Y. Jiang, L. Song and X. Wang (2009). "Comparison of in vitro hormone activities of selected phthalates using reporter gene assays." *Toxicology Letters* **191**(1): 9-14.

Shiraki, T., N. Kamiya, S. Shiki, T. S. Kodama, A. Kakizuka and H. Jingami (2005). "α, β-unsaturated ketone is a core moiety of natural ligands for covalent binding to peroxisome proliferator-activated receptor γ." *Journal of Biological Chemistry* **280**(14): 14145-14153.

Shu, H., B. A. Jönsson, M. Larsson, E. Nånberg and C. G. Bornehag (2014). "PVC flooring at home and development of asthma among young children in Sweden, a 10-year follow-up." *Indoor Air* **24**(3): 227-235.

Sica, A. and A. Mantovani (2012). "Macrophage plasticity and polarization: in vivo veritas." *The Journal of Clinical Investigation* **122**(3): 787-795.

Silva, M. J., D. B. Barr, J. A. Reidy, N. A. Malek, C. C. Hodge, S. P. Caudill, J. W. Brock, L. L. Needham and A. M. Calafat (2004). "Urinary levels of seven phthalate metabolites in the US population from the National Health and Nutrition Examination Survey (NHANES) 1999-2000." *Environmental Health Perspectives* **112**(3): 331–338.

Silverthorn, D. U. (2015). "Human Physiology: An Integrated Approach", 7th edition. England, Pearson Education.

Standiford, T. J., V. G. Keshamouni and R. C. Reddy (2005). "Peroxisome proliferator-activated receptor-γ as a regulator of lung inflammation and repair." *Proceedings of the American Thoracic Society* **2**(3): 226-231.

Steensen, T. B. (2016). "The effects of di-n-Butyl Phthalate (DBP) on human primary immune cells." Master thesis, University of Oslo.

Subrata, L. S., J. Bizzintino, E. Mamessier, A. Bosco, K. L. McKenna, M. E. Wikström, J. Goldblatt, P. D. Sly, B. J. Hales and W. R. Thomas (2009). "Interactions between innate antiviral and atopic immunoinflammatory pathways precipitate and sustain asthma exacerbations in children." *The Journal of Immunology* **183**(4): 2793-2800.

Takeuchi, S., M. Iida, S. Kobayashi, K. Jin, T. Matsuda and H. Kojima (2005). "Differential effects of phthalate esters on transcriptional activities via human estrogen receptors α and β, and androgen receptor." *Toxicology* **210**(2): 223-233.

Tanaka, A., A. Matsumoto and T. Yamaha (1978). "Biochemical studies on phthalic esters. III. Metabolism of dibutyl phthalate (DBP) in animals." *Toxicology* **9**(1): 109-123.

Teixeira, D., C. Marques, D. Pestana, A. Faria, S. Norberto, C. Calhau and R. Monteiro (2015). "Effects of xenoestrogens in human M1 and M2 macrophage migration, cytokine release, and estrogen-related signaling pathways." *Environmental Toxicology* **31**(11): 1496-1509.

ThermoFisher (2016). "alamarBlue®—Rapid & Accurate Cell Health Indicator." Retrieved 19/8, 2016, from https://www.thermofisher.com/no/en/home/brands/molecular-probes/key-molecular-probes-products/alamarblue-rapid-and-accurate-cell-health-indicator.html.

Tontonoz, P., L. Nagy, J. G. Alvarez, V. A. Thomazy and R. M. Evans (1998). "PPARγ promotes monocyte/macrophage differentiation and uptake of oxidized LDL." *Cell* **93**(2): 241-252.

Towbin, H., T. Staehelin and J. Gordon (1979). "Electrophoretic transfer of proteins from polyacrylamide gels to nitrocellulose sheets: procedure and some applications." *Proceedings of the National Academy of Sciences* **76**(9): 4350-4354.

Tsuchiya, S., M. Yamabe, Y. Yamaguchi, Y. Kobayashi, T. Konno and K. Tada (1980). "Establishment and characterization of a human acute monocytic leukemia cell line (THP-1)." *International Journal of Cancer* **26**(2): 171-176.

Uppenberg, J., C. Svensson, M. Jaki, G. Bertilsson, L. Jendeberg and A. Berkenstam (1998). "Crystal structure of the ligand binding domain of the human nuclear receptor PPARγ." *Journal of Biological Chemistry* **273**(47): 31108-31112.

Uray, I. P., Y. Liang and S. M. Hyder (2004). "Estradiol down-regulates CD36 expression in human breast cancer cells." *Cancer Letters* **207**(1): 101-107.

Vats, D., L. Mukundan, J. I. Odegaard, L. Zhang, K. L. Smith, C. R. Morel, D. R. Greaves, P. J. Murray and A. Chawla (2006). "Oxidative metabolism and PGC-1β attenuate macrophage-mediated inflammation." *Cell Metabolism* **4**(1): 13-24.

Waku, T., T. Shiraki, T. Oyama, Y. Fujimoto, K. Maebara, N. Kamiya, H. Jingami and K. Morikawa (2009). "Structural insight into PPARγ activation through covalent modification with endogenous fatty acids." *Journal of Molecular Biology* **385**(1): 188-199.

Waku, T., T. Shiraki, T. Oyama, K. Maebara, R. Nakamori and K. Morikawa (2010). "The nuclear receptor PPARγ individually responds to serotonin-and fatty acid-metabolites." *The EMBO journal* **29**(19): 3395-3407.

Wang, G., R. Cao, Y. Wang, G. Qian, H. C. Dan, W. Jiang, L. Ju, M. Wu, Y. Xiao and X. Wang (2016). "Simvastatin induces cell cycle arrest and inhibits proliferation of bladder cancer cells via PPARγ signalling pathway." *Scientific Reports* **6**: 35783. doi:35710.31038/srep35783.

Weschler, C. J., G. Bekö, H. M. Koch, T. Salthammer, T. Schripp, J. Toftum and G. Clausen (2015). "Transdermal uptake of diethyl phthalate and di (n-butyl) phthalate directly from air: experimental verification." *Environmental Health Perspectives* **123**(10): 928-934.

Whyatt, R. M., M. S. Perzanowski, A. C. Just, A. G. Rundle, K. M. Donohue, A. M. Calafat, L. A. Hoepner, F. P. Perera and R. L. Miller (2014). "Asthma in inner-city children at 5–11 years of age and prenatal exposure to phthalates: the Columbia Center for Children's Environmental Health Cohort." *Environmental Health Perspectives* **122**(10): 1141-1146.

Wittassek, M. and J. Angerer (2008). "Phthalates: metabolism and exposure." *International Journal of Andrology* **31**(2): 131-138.

Wittassek, M., H. M. Koch, J. Angerer and T. Brüning (2011). "Assessing exposure to phthalates–the human biomonitoring approach." *Molecular Nutrition & Food Research* **55**(1): 7-31.

Woo, M.-S., J. Yang, C. Beltran and S. Cho (2016). "Cell Surface CD36 Protein in Monocyte/Macrophage Contributes to Phagocytosis during the Resolution Phase of Ischemic Stroke in Mice." *Journal of Biological Chemistry* **291**(45): 23654-23661.

Wormuth, M., M. Scheringer, M. Vollenweider and K. Hungerbühler (2006). "What are the sources of exposure to eight frequently used phthalic acid esters in Europeans?" *Risk Analysis* **26**(3): 803-824.

Wynn, T. A., A. Chawla and J. W. Pollard (2013). "Macrophage biology in development, homeostasis and disease." *Nature* **496**(7446): 445-455.

Xu, H., X. Shao, Z. Zhang, Y. Zou, X. Wu and L. Yang (2013). "Oxidative stress and immune related gene expression following exposure to di-n-butyl phthalate and diethyl phthalate in zebrafish embryos." *Ecotoxicology and Environmental Safety* **93**: 39-44.

Xue, J., S. V. Schmidt, J. Sander, A. Draffehn, W. Krebs, I. Quester, D. De Nardo, T. D. Gohel, M. Emde and L. Schmidleithner (2014). "Transcriptome-based network analysis reveals a spectrum model of human macrophage activation." *Immunity* **40**(2): 274-288.

Yessoufou, A. and W. Wahli (2010). "Multifaceted roles of peroxisome proliferator-activated receptors (PPARs) at the cellular and whole organism levels." *Swiss Medical Weekly* **140**: w13071. doi:13010.14414/smw.12010.13071.

Zaas, A. K. and D. A. Schwartz (2005). "Innate immunity and the lung: defense at the interface between host and environment." *Trends in Cardiovascular Medicine* **15**(6): 195-202.

Appendix 1: Detailed information regarding products, reagents, chemicals and equipment

Reagent	Supplier
15-Deoxy-Δ12,14-prostaglandin J2	Sigma Aldrich, St. Louis, MO, USA
30% Acrylamide/Bis Solution	BIO-RAD, Hercules, California, USA
AlamarBlue	Invitrogen, Thermo Fisher Scientific, Waltham, Massachusetts, USA
Ammonium persulphate	BIO-RAD, Hercules, California, USA
Aprotein (A-1153)	Sigma Aldrich, St. Louis, MO, USA
B-mercaptoethanol	Sigma Aldrich, St. Louis, MO, USA
Bovine serum albumin	Sigma by life technologies, Thermo fisher scientific, Waltham, Massachusetts, USA
Dulbecco's Phosphate-Buffered Saline	Folkehelseinstituttet Substratlab.
EDTA	Sigma Aldrich, St. Louis, MO, USA
EGTA	Sigma Aldrich, St. Louis, MO, USA
Gentamicine	Gibco by life technologies, Thermo fisher scientific, Waltham, Massachusetts, USA
Glycerol	Merck, Whitehouse Station, NJ, USA
GW9662	Cayman Chemical, Ann Arbor, Michigan, USA
Hepes	Sigma Aldrich, St. Louis, MO, USA
HI foetal bovine serum	Gibco by life technologies, Thermo fisher scientific, Waltham, Massachusetts, USA
Human Truestain FcX	BIO-RAD, Hercules, California, USA
LDH concentrate solution (L2500-5KU, L-lactic dehydrogenase from rabbit muscle)	Sigma Aldrich, St. Louis, MO, USA
Leupeptin (L-2884)	Sigma Aldrich, St. Louis, MO, USA

Pepsatin A (P-5318)	Sigma Aldrich, St. Louis, MO, USA
Phorbol myristate acetate	Sigma Aldrich, St. Louis, MO, USA
PMSF	Sigma Aldrich, St. Louis, MO, USA
Poncheu S	Sigma Aldrich, St. Louis, MO, USA
Precision Plus Protein™ Dual Xtra Standard	BIO-RAD, Hercules, California, USA
Rosiglitazone	Cayman Chemical, Ann Arbor, Michigan, USA
RPMI 1640 with L-glutamine	BioWhittaker, Lonza, Belgium (Basel, Switzerland)
Skim milk powder	Fluka analytical, Sigma Aldrich, St. Louis, MO, USA
Sodium azide solution	Folkehelseinstituttet Substratlab.
Sodium chlodride	Merck, Whitehouse Station, NJ, USA
Sodium dodecyl sulphate	Fluka, Sigma Aldrich, St. Louis, MO, USA
Sodium fluoride	Riedel-de Haën, Sigma Aldrich, St. Louis, MO, USA
Sodium orthovanadate	Sigma Aldrich, St. Louis, MO, USA
Sodium Pyrophosphate	Sigma Aldrich, St. Louis, MO, USA
Sodium Pyruvate	Sigma Aldrich, St. Louis, MO, USA
Stempro accutase	Gibco by life technologies (thermo fisher scientific?), Cambridge, UK
Sulfosalicylic acid	Sigma Aldrich, St. Louis, MO, USA
TEMED	BIO-RAD, Hercules, California, USA
Trichloro acetic acid	Sigma Aldrich, St. Louis, MO, USA
Triton X-100	Sigma Aldrich, St. Louis, MO, USA
Trizma base	Sigma Aldrich, St. Louis, MO, USA
Trizma hydrochloride	Sigma Aldrich, St. Louis, MO, USA
Tween 20	Sigma Aldrich, St. Louis, MO, USA

Kit	Supplier
ab113474 - Nuclear extraction kit	Abcam, Cambridge, UK
ab133101 - PPAR gamma Transcription Factor Assay Kit	Abcam, Cambridge, UK
Cytotoxicity Detection Kit^{PLUS} (LDH)	Roche, Sigma Aldrich, St. Louis, MO, USA
DC™ Protein Assay	BIO-RAD, Hercules, California, USA
SuperSignal™ West Dura Extended Duration Substrate	Thermo Fisher Scientific, Waltham, Massachusetts, USA

Antibody	Supplier
Anti-HDAC1 antibody	Abcam, Cambridge, UK
GAPDH (14C10) Rabbit mAb	Cell signalling technology, Danvers, Massachusetts, USA
Mouse anti-human CD36:Alexa Fluor® 647	AbD Serotec, BIO-RAD, Hercules, California, USA
Polyclonal Goat Anti-Rabbit Immunoglobulin/HRP	Dako, Denmark

Cell line	Supplier
THP-1	ECACC, Sigma Aldrich, St. Louis, MO, USA

Software	Supplier
BD FacsDiva	BD biosciences, San Jose, California, USA
Excel 2013 for Windows	Microsoft, Redmond, Washington, USA
FCS Express V3	De Novo Sofware, Los Angeles, California, USA
Graphpad Prism 5 for Windows (version 5.4)	GraphPad Software Inc., La Jolla, California, USA
Image Lab™	BIO-RAD, Hercules, California, USA

Magellan 4	TECAN, Männedorf, Switzerland
MARS data analysis software V3	BMG Labtech, Ortenberg, Germany

Equipment	Supplier
BD LSR II flow cytometer	BD biosciences, San Jose, California, USA
Bioruptor Plus sonication device	Diagenode, Liége, Belgium
ChemiDoc™ XRS+ molecular imager	BIO-RAD, Hercules, California, USA
CLARIOstar plate reader	BMG Labtech, Ortenberg, Germany
Galaxy S+ incubator	RS biotech, Irvine, UK
Labculture Class II Type A2 biological safety cabinet	Esco technologies, Horsham, Pennsylvania, USA
Luna II automated cell counter	Logos biosystems, Dongan-gu Anyang-si, South Korea
Sunrise remote plate reader	TECAN, Männedorf, Switzerland

Laboratory equipment	Supplier
1.5 mL Micro tubes (Eppendorf tubes)	BRAND, Wertheim, Germany
15 ml tubes	VWR, Radnor, Pennsylvania, USA
50 ml tubes	VWR, Radnor, Pennsylvania, USA
BD Falcon tubes	BD biosciences, San Jose, California, USA
Corning™ Costar™ Flat Bottom Cell Culture Plates (6 well, 12 well and 24 well)	Fisher Scientific Hampton, New Hampshire, USA
Microtest plate	Sarstedt, Nümbrecht, Germany
Nitrocellulose blotting membrane	GE Healthcare Life Sciences, Chicago, Illinois, USA
Nunc EasyFlask™ 75 cm^2 cell culture flask	Thermo Fisher Scientific, Waltham, Massachusetts, USA
Nunc Maxisorb plate	Thermo Fisher Scientific, Waltham, Massachusetts, USA

Appendix 2: Solutions and buffers

Cells and exposure

Cell culture medium

RPMI 1640 with L-glutamine	500 mL
Sodium pyruvate	55 mg
Hepes (pH 7.3)	5.5 mL
Gentamicin (50 ng/mL)	0.55 mL
HI foetal bovine serum	55 mL (110 mL*)

Medium containing 20% FBS was used to aliquot and thaw the cells.

Flow cytometry

Flow cytometry staining buffer

Dulbecco's Phosphate-Buffered Saline	500 mL
Bovine serum albumin	2.5 g
Sodium azide solution	0.5 mL

Nuclear extraction

1X pre-extraction buffer

Dilute Pre-Extraction buffer (10X) at a 1:10 ratio in distilled H_20.
Add DTT solution and PIC to 1X Extraction Buffer at a 1:1000 ratio.

Extraction buffer

Add DTT solution and PIC to Extraction Buffer at a 1:1000 ratio.

PPARγ activation

Complete transcription factor binding assay buffer (CTFB)

Volume/well

Distilled H_20	73 µL
Transcription factor Binding Assay Buffer (4x)	25 µL
Reagent A	1 µL
300 mM DTT	1 µL

Transcription factor antibody binding buffer (ABB)

Dilute ABB (10X) 1:10 in distilled H_20.

Wash buffer

Dilute wash buffer concentrate (400X) 1:400 in distilled H_20.
Add Polysorbate 20 to wash buffer (0.5 mL/Litre wash buffer).

Western blotting

SDS Buffer

Sodium dodecyl sulphate	2 g
0.5 M Tris-HCL, pH 6.8	12.5 mL
Marcaptoethanol	5 mL
1% Bromphenolblue	1 mL
Distilled H_2O	20 mL

Lysis buffer

0.5 M Tris pH 7.5	6 mL
NaCl	1.32 g
0.5 M EDTA	0.3 mL
EGTA	57 mg
Sodium pyrophosphate	167 mg
β-glycerolphosphate	32.4 mg
Sodium orthovanadate	27.6 mg
0.5 M sodium fluoride	0.3 mL
Triton X-100	1.5 mL
Distilled H_2O	30 mL

Before use, dilute 1:5 in distilled H_2O and add:
10 µg/mL leupeptin
1 mM PMSF
10 µg/mL Pepsatin A
10 10 µg/mL aprotein

12% polyacrylamide gel

Distilled H_20	3.3 mL
30% Acrylamide Solution	4.0 mL
1.5 M Tris (pH 8.8)	2.5 mL
10% SDS	0.1 mL
10% APS	0.1 mL
TEMED	0.004 mL

Stacking gel

Distilled H_20	6.1 mL
0.5M Tris-HCL (pH 6.8)	2.5 mL
10% SDS	0.1 mL
30% Acrylamide Solution	1.3 mL
10% APS	0.05 mL
TEMED	0.01 mL

Electrophoresis buffer (10x)

Trizma base	30 g
Glycine	144 g
SDS	10 g
Distilled H_20	1000 mL

Before use, dilute 1:10 using distilled H_20

Transfer buffer (10x)

Trizma base	30 g
Glycine	144 g
Distilled H_20	1000 mL

Before use, add 200 mL methanol and 700 mL distilled H_20 to 100 mL transfer buffer (10x).

Ponceu S colour solution

Ponceau S	2 g
Trichloro acetic acid	30 g
Sulfosalicylic acid	30 g
Distilled H_20	1000 mL

Wash buffer

Trizma base	12 g
NaCl	80 g
Tween-20	10 mL
Distilled H_20	1000 mL

3% Dry milk

Skim milk powder	3 g
Wash buffer	100 mL

5% Bovine serum albumin

Bovine serum albumin	5 g
Wash buffer	100 mL

0.5M Tris-HCL (pH 6.8)

Trizma hydrochloride	17.5 g
Trizma base	1.7 g
Distilled H_20	250 mL

1.5M Tris-HCL (pH 8.8)

Trizma hydrochloride	9.23 g
Trizma base	38.5 g
Distilled H_20	250 mL

10% SDS

Sodium dodecyl sulphate	10 g
Distilled H_20	100 mL

10% APS

Ammonium persulfate	100 mg
Distilled H_20	1 mL

Appendix 3: Incubation time for alamarBlue

Several time points were tested to determine the optimal incubation time for the alamarBlue assay. For the initial experiments fluorescence was detected at 30 minutes, 60 minutes, 90 minutes and 120 minutes. The difference in fluorescence intensity was greatest between 30 minutes and 60 minutes incubation time, and seemed to reach a plateau between 60 minutes and 90 minutes (Figure 13) or 90 minutes and 120 minutes (not shown) for the individual experiments. This indicated that there was still sufficient substrate available after 60 minutes incubation. Consequently, samples were incubated for 60 minutes prior to detection of fluorescence for the remainder of the experiments.

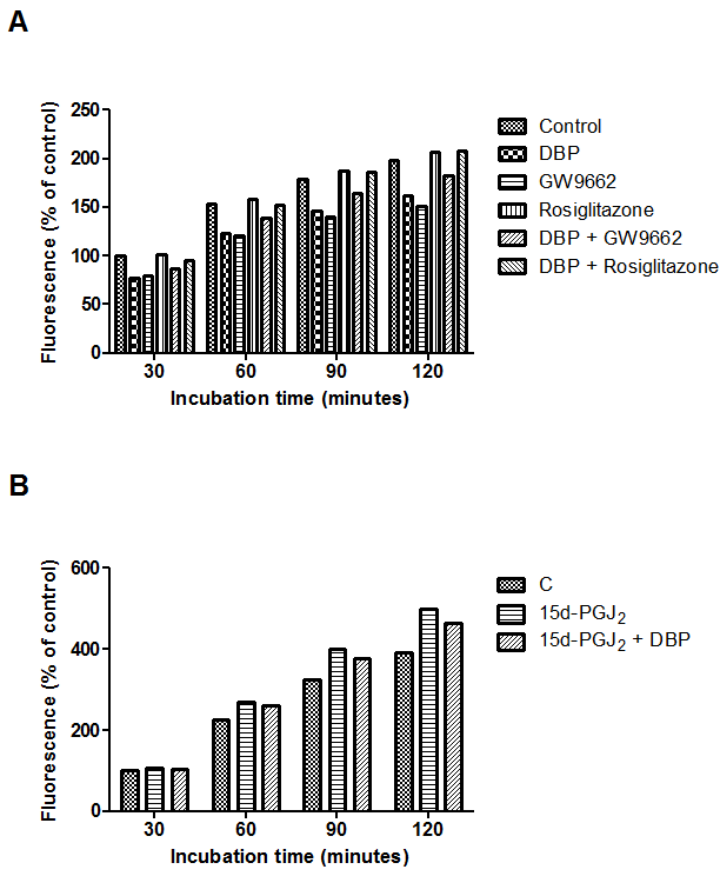

Figure 13. *Fluorescence for the same samples at different points of time. (A and B)* THP-1 cells were exposed to rosiglitazone (0.5 µM), GW9662 (10 µM), DBP (80 µM) and 15d-PGJ_2 (1 µM) for 24 hours, either alone or in combination, prior to 48-hour exposure to PMA (Exposure regime I). After addition of alamarBlue reagent, the samples were incubated for a total 120 minutes with fluorescence being measured after 30 minutes, 60 minutes, 90 minutes and 120 minutes. Data is derived from one representative experiment and is presented as a percentage of the control after 30 minutes incubation.

Appendix 4: PPARγ activation assay

The PPARγ activation assay (PPAR gamma Transcription Factor Assay Kit, Abcam) was performed to supplement the conclusions based on the expression of CD36. The following appendix contains the methods for the nuclear extraction procedure (4.1) and PPARγ activation assay (4.2), the results derived from the assay (4.3) and the discussion of these results (4.4).

4.1 Exposure and preparation of the nuclear extracts

Cells were seeded on 6 well cell culture plates and exposed according to exposure regime I and II (section 3.3.2). The stock solutions and the final concentrations of DBP rosiglitazone and 15d-PGJ_2 in the well were the same as described in section 3.3.3. The reagents, chemicals, equipment, solutions and buffers used in the procedure described below is listed in Appendix 1 and Appendix 2.

The nuclear extracts were prepared using a nuclear extraction kit, applied according to the manufacturers recommendations. Following exposure, the cells were transferred to 15 ml conical tubes and quantified using a LUNA II automated cell counter. The cells were then centrifuged for 5 minutes at 1000 rpm and the supernatant discarded. The pellet was re-suspended in PBS so that the concentration of cells in each sample was approximately $2x10^6$ cells/mL. The number of cells required for the rest of the procedure ($3x10^6$) was subsequently transferred to 1.5 mL eppendorf tubes, centrifuged for 5 minutes at 1000 rpm and the supernatant discarded. To lyse the cells the pellet was re-suspended in 100 µL chilled pre-extraction buffer per 10^6 cells and incubated on ice for 10 minutes. The sample was then vortexed for 10 seconds and immediately centrifuged for 1 minute at 12000 rpm. The supernatant, now containing the cytosolic fraction, was carefully removed and transferred to new eppendorf tubes. The nuclear pellet was re-suspended in extraction buffer containing DTT solution and PIC at a 1:1000 ratio, using 10 µL extraction buffer per 10^6 cells. The nuclear samples were incubated on ice for 15 minutes with 5 seconds vortex every 3 minutes. To further lyse the nuclei, sonication was performed using a Bioruptor® Plus sonication device for three cycles of ten seconds. Finally, nuclear proteins were extracted by centrifuging the suspension for 10 minutes at 12000 rpm. The supernatants, now containing the nuclear

fraction of the cells, were carefully removed from the pellet and transferred to new 0.5 mL eppendorf tubes.

The protein concentrations of the extracts were determined using a DC™ Protein Assay kit, according to the manufacturers instructions. The protein standard was diluted in a series yielding eight concentrations spanning from 0-20 mg/mL. The protein extract samples were either used undiluted or diluted two times, depending on the amount of sample available. Then, 5 µL of undiluted sample or diluted standard was added to the wells of a microtiter plate. Subsequently, 25 µL of working reagent A`, consisting of 98% solution A and 2% solution S, was added to each well. Finally, 200 µL of reagent B was added to each well, before the plate was incubated in darkness at room temperature for 15 minutes. The resulting absorbance was read at 750 nm using a Sunrise absorbance reader.

The separation of the nuclear and cytosolic fractions was assessed using western blotting, an analytical method using electrophoresis separate the proteins in a sample in a polyacrylamide gel and transfer them to a nitrocellulose membrane (NC), followed by detection using antibody staining (Towbin *et al.* 1979, Burnette 1981). The separation of the two fractions was assessed by staining for proteins that are only found in one fraction or the other. Histone deacetylase 1 (HDAC1) was used as an indicator for the nuclear fraction, while glyceraldehyde 3-phosphate dehydrogenase (GAPDH) was used for the cytosolic fraction. The presence of HDAC1 in the cytosolic samples and GAPDH in the nuclear samples would indicate an imperfect separation of the two fractions.

Gel electrophoresis using a 12% polyacrylamide gel was applied to separate the proteins in the samples. The gel was composed of two different parts, a stacking gel, in which the samples were applied, and a separation gel through which the proteins were separated. The gels were cast to a thickness of 1.5 mm between plates of glass in gel solidification racks. The separation gel was mixed first and allowed to polymerize for 30-45 minutes. Isopropanol was applied to the top of the gel to even it out and remove bubbles. Once the gel was sufficiently polymerized the isopropanol was rinsed off with distilled water and the stacking gel applied. A comb was inserted to form wells before the gel was allowed to polymerize for 30 minutes. The comb was then carefully removed and the gel placed in an electrophorator filled with electrophoresis buffer. Based on the concentrations obtained from the protein assay all samples were diluted to the same

protein concentration using SDS buffer, lysis buffer and glycerol. The samples and Precision Plus Protein Dual Xtra Standard were then applied to the wells and a power source connected. The electrophoresis was first run at 100 V to collect the samples in the wells before increasing it to 200 V to separate the proteins. After sufficient separation had been achieved the electrophoresis chamber was taken apart, the stacking gel discarded and the separation gel placed in transfer buffer.

Prior to the blotting procedure, the blotting cassette, NC membrane, filter paper and sponges of correct size were soaked in transfer buffer. The filter paper, NC membrane and sponges were then assembled in the blotting cassette, in the order sponge, filter paper, gel, nitrocellulose membrane, filter paper and sponge, taking care to remove any bubbles trapped between the layers. After assembly the cassette was placed in an electrophorator filled with cold transfer buffer. A block of ice and a magnetic stirrer were placed in the chamber to provide circulation and to keep it cool. A power source was then applied forming an electrical field with the NC membrane facing the positive side. The blotting ran for 60-90 minutes at 70 V, transferring the proteins from the gel to the NC membrane. After the blotting was finished the electrophorator and the blotting cassette were disassembled, and the membrane was put in Ponceu S colour for 2 minutes to visualize the protein bands. Excess colour was rinsed of using tap water and the membrane scanned on a computer using a ChemiDoc™ XRS+ molecular imager with Image Lab™ software.

Prior to immunodetection, the blots were incubated with a 3% dry milk solution for 30 minutes at room temperature to prevent non-specific interactions between the NC membrane and the antibodies. The membrane was then incubated with primary antibody solution overnight with gentle tilting at 4°C. Both the rabbit anti-HDAC1 and the rabbit anti-GAPDH antibodies were diluted in a 5% bovine serum albumin (BSA) solution to a ratio of 1:2000 and 1:2500, respectively. Following incubation, the membrane was washed three times for 10 minutes using wash buffer to remove excess antibodies, changing the wash buffer between each cycle. To detect the proteins the membrane was incubated for 2 hours at room temperature with goat anti-rabbit antibody conjugated with horseradish peroxidase (HRP), diluted 1:1000 in 3% dry milk solution. To remove excess secondary antibody solution the membrane was washed three times for 10 minutes using wash buffer. A 1:1 solution of Peroxidase buffer and

Luminol/Enhancer solution from a Supersignal® West Dura Extended Duration Subrate kit was then prepared. The membrane was placed in the solution for 5 minutes, ensuring even coverage by continuously pipetting the solution over the membrane. Chemiluminescence was then detected using a ChemiDoc™ XRS+ molecular imager with Image Lab™ software.

4.2 Detection of activated PPARγ

Activated PPARγ in the nuclear extracts was detected using a PPAR gamma Transcription Factor Assay kit, applied according to the manufacturers manual. The assay is colorimetric, using a 96 well plate pre-coated with a double stranded DNA (dsDNA) sequence containing the peroxisome-proliferator response element (PPRE). Activated PPARγ in the extracts bind specifically to the PPRE and are detected by adding a specific primary anti-PPARγ antibody followed by a secondary antibody conjugated with HRP providing a colorimetric readout at 450 nm. Each sample and control was added to pre-determined wells together with complete transcription factor binding assay buffer (CTFB) to a total volume of 100 µL. In sample wells or wells designated positive control, 90 µL CTFB was added followed by 10 µL of nuclear extract sample or 10 µl positive control solution. 100 µL CTFB was added to blank wells or wells designated as control for non-specific binding of the primary antibody. The plate was then sealed using an adhesive cover and incubated at 4°C overnight without agitation to allow active PPARγ in the sample to bind to the PPRE. After the incubation, the wells were emptied and washed five times using 200 µL wash buffer to remove any unbound reagents. The wells were emptied after each wash. Following the final wash, the plate was tapped on a paper towel in order to remove any remaining wash buffer. The transcription factor PPAR gamma primary antibody was diluted 1:100 in transcription factor antibody binding buffer (ABB) and 100 µL added to each well except the blank. The plate was sealed using an adhesive cover and incubated for one hour at room temperature without agitation. Any unbound primary antibody was then removed by washing the wells five times with 200 µL wash buffer.

The transcription factor goat anti-rabbit HRP-conjugate secondary antibody was diluted 1:100 in ABB and 100 µL added to each well except the blank. The plate was then incubated for another hour at room temperature without agitation, using an adhesive cover to seal the plate. Following the incubation the wells were washed five times with

200 µL wash buffer to remove unbound secondary antibody. A colorimetric reaction was started by adding 100 µL transcription factor developing solution to each well. The plate was subsequently incubated for 45 minutes at room temperature with gentle agitation. Following incubation, 100 µL of stop solution was added to each well to end the reaction, changing the colour from blue to yellow. Finally, absorbance was read at 450 nm.

4.3 Results

Western blotting using antibodies recognizing proteins exclusive to either the nuclear or cytosolic fraction was applied as a control for the nuclear extraction procedure. When stained with antibodies recognizing HDAC1, a nuclear protein, nuclear samples exhibited stronger bands than cytosolic samples (Figure 14A). Conversely, there were stronger bands in cytosolic samples compared with nuclear samples when staining with an antibody recognizing the cytosolic protein GAPDH (Figure 14B). Although, faint bands occurred in lanes containing nuclear samples when staining with GAPDH, indicating slight contamination of the nuclear extract (Figure 14B), these results suggest that the nuclear extraction procedure was successful.

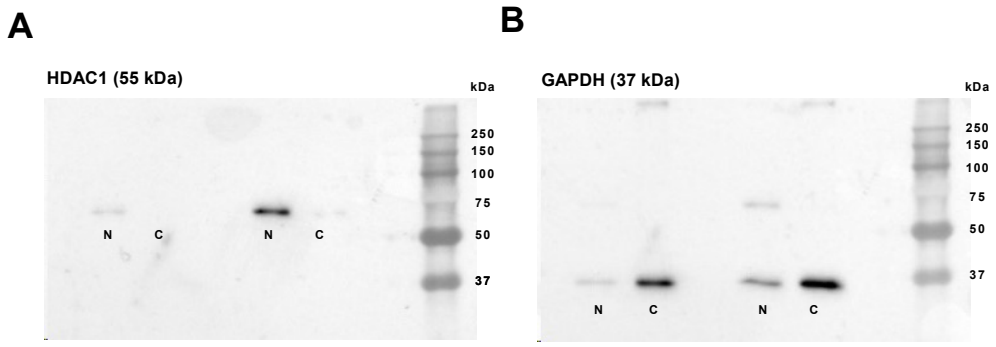

Figure 14. *Western blots of the nuclear and cytosolic fractions.* The separation of the nuclear (N) and cytosolic (C) fractions was assessed using western blotting. The blot was stained with antibodies for either the nuclear protein HADC1 (A) or the cytosolic protein GAPDH (B).

Different exposure regimes were attempted to establish that PPARγ was activated in the applied cell culture system (Figure 15A). Cells were exposed to rosiglitazone or 15d-PGJ_2 for either 3 hours (Figure 15Aa) or 24 hours (Figure 15Ab). However, neither rosiglitazone nor 15d-PGJ_2 appeared to activate PPARγ over control level after 3 hours (Figure 15B) or 24 hours (Figure 15C) exposure. To assess if differentiating the cells into macrophages would affect the results, the cells were treated with PMA for 3 hours

(Figure 15Ac), 24 hours (Figure 15Ad) or 48 hours (Figure 15Ae), after exposure to either rosiglitazone or 15d-PGJ_2. However, PMA-induced differentiation did not alter the outcome (Figure 15D-F).

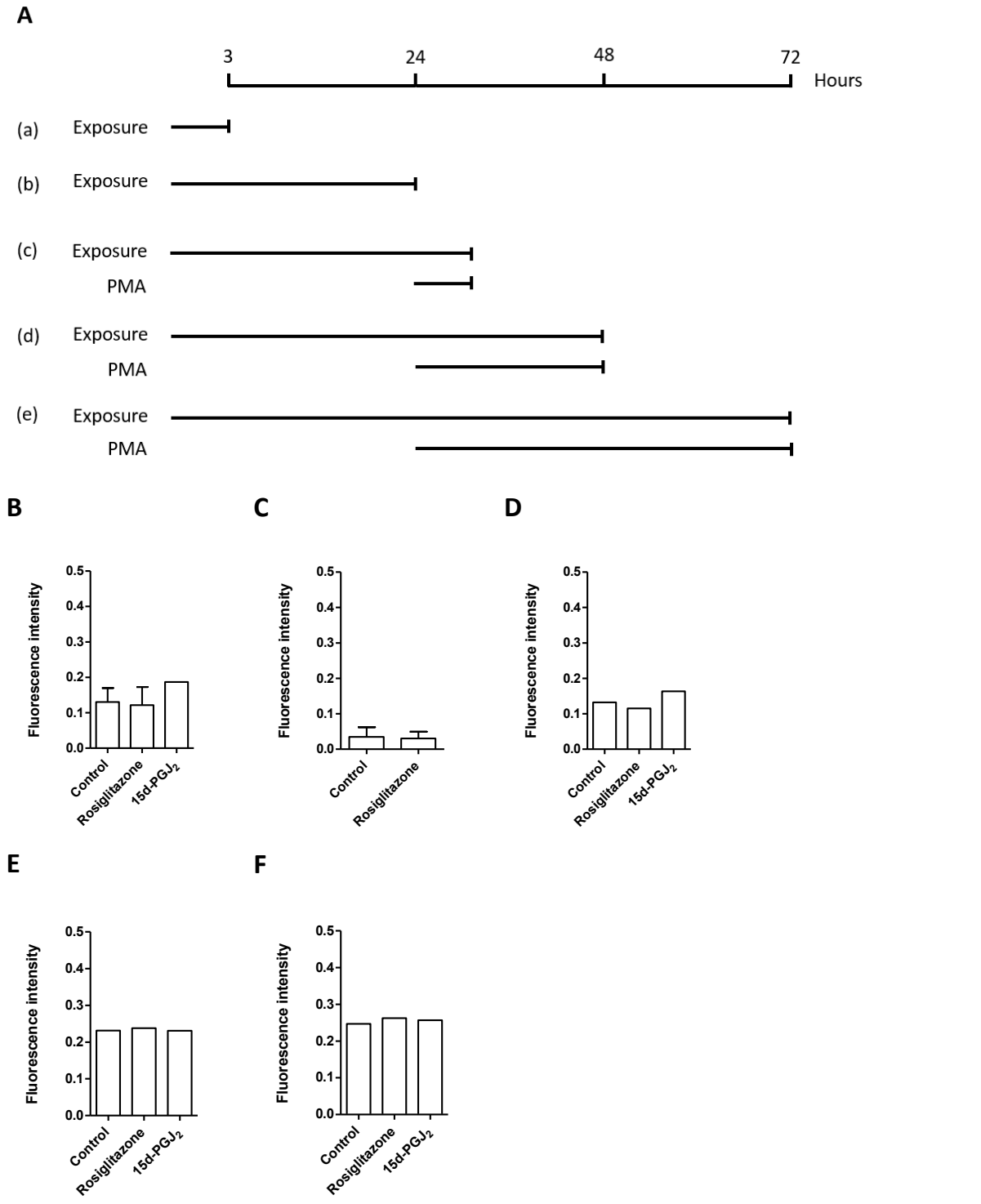

Figure 15. *Troubleshooting of the PPARγ activation assay*. A: Overview of the exposure regimes used in the applied model system. B-F: Cells were exposed to 0.5 µM rosiglitazone (B-F) or 5.0 µM 15d-PGJ_2 (B, E and F) for either 3 hours (B) or 24 hours (C-F). E and F: Differentiation into macrophage-like cells was induced by treatment with PMA for 3 (D), 24 (E) or 48 hours (F) after exposure to rosiglitazone or 15d-PGJ_2. Values represent the fluorescence intensity of the samples at 450 nm.

4.4 Discussion

In the present study, the state of PPARγ activation in the nuclear extracts of THP-1 monocytes and THP-1 macrophages was no different from control after treatment with rosiglitazone and 15d-PGJ_2. The lack of positive effects were not due to methodological error, as the western blots of the nuclear extracts indicated adequate separation of the nuclear and cytosolic fractions, and the positive control provided with the PPARγ activation assay kit resulted in the expected OD of 0.8-1.5 (data not shown).

Another possibility is that the assay was not suitable for our model system. The activation of PPARγ and the subsequent binding to the PPRE involves the association and dissociation with various cofactors, post-translational modification and dimerization with RXR-α (Kim *et al.* 2013). If the activated PPARγ complexes were not intact following the procedure, and thus unable to bind to DNA, it would result in a lack of PPARγ activation in the applied assay. Alternatively, it may be that the DNA coating of the wells contains a PPRE region of a promoter sequence not recognized by the activated PPARγ complex induced by the experimental treatments in the model system used in the present study.

A third possibility is that the tested exposure regimes and time points were not optimal for detecting PPARγ activation. Cells were harvested after either 3 hours or 24 hours. Consequently, if PPARγ has a narrow peak of activation prior to the 3-hour mark, it is a possibility that the chosen time points of the present study missed the peak of activation. However, this scenario seems unlikely, as a robust activation of PPARγ has been reported after 4-48 hours for other cellular model systems and stimuli, using the same assay as applied in the present study (Samokhvalov *et al.* 2014, Wang *et al.* 2016) or an alternative similar assay (Hasegawa *et al.* 2007, Bruyère *et al.* 2011).

Since activated PPARγ could not be detected after exposure in the current experimental setup, it is possible that rosiglitazone and 15d-PGJ_2 do not act as PPARγ agonists in the applied model system and that the observed effects on CD36 are independent of PPARγ. However, given the status of CD36 as a PPARγ-controlled gene in macrophages in addition to rosiglitazone and 15d-PGJ_2 being established PPARγ agonists (Tontonoz *et al.* 1998, Chawla *et al.* 2001), this scenario seems unlikely. Moreover, both agonists induced a robust increase in CD36 expression, strongly suggesting that PPARγ is

activated. Consequently, the results obtained from the analysis of CD36 are considered more credible as evidence than the PPARγ activation assay.

As we were unable to detect PPARγ activation by rosiglitazone and 15d-PGJ_2, it was decided not to use DBP in this assay. However, DBP enhanced the expression of CD36 and modulated the effect of rosiglitazone and 15d-PGJ_2, indicating that DBP interacts with PPARγ (See main discussion section 5.2 for details). Further support is provided by a SILAC (stable isotope labelling with amino acids in cell culture) assay performed previously in our lab, where 4 out of 7 proteins detected to be increased by DBP in the applied cell model were regulated by PPARγ, further supporting a role of PPARγ in the observed effects (unpublished data).